Model-aided understanding of competitor-mediated coexistence

Doctoral Thesis

Model–Aided Understanding of Competitor–Mediated Coexistence

(競争緩和共存のモデル支援解析)

Makoto Tohma

Graduate School of Advanced Mathematical Sciences,
Meiji University

Supervisor: Professor Masayasu Mimura

2013/Feb/12

Abstract

This thesis theoretically tackles a coexistence of competing species problem in mathematical ecology, that is, "Even if some species which are competing with others are weaker, can they coexist with the stronger species in competiton for some reason?" If so, it is called the competitor-mediated coexistence. This is a very important ecological problem, because it closely correlates with species diversity. The starting point of theoretical research on species diversity could be the law of competitive exclusion, which was proposed by the Russian ecologist, G. Gause ([10]). The law can be summarized as follows: "Two species strongly competing for the same resources cannot coexist if other ecological factors are constant." However, the coexistence of strongly competing species can be observed in nature, and such coexistence plays an important role in species diversity. Therefore, the occurrence of competitor-mediated coexistence would be one of the reasons for species diversity.

From the viewpoint of competitor-mediated coexistence, it is important to study the influence of exotic species on other native ones as exogenous effect. In general, exotic species are not necessarily stronger and may be weaker than native ones because they have evolved in a different ecological environment ([17]). But even if exotic species is weaker, it might cooperate with weaker native species after which the cooperation might reverse competitive relations among native species. This gives us the following question: Whether or not competitor-mediated coexistence can occur by a invasion of weaker exotic species?

This thesis is to consider the ecological situation where one exotic competing species invades the native system of two strongly competing species and discusses this problem theoretically using a three species competition-diffusion sys-

tems which is often used in mathematical ecology.

This thesis is composed of nine chapters and one appendix. The organization of this thesis is as follows: In Chapter 1, I show earlier studies and clarified the position of this thesis.

In Chapter 2, I first introduce a three species competition–diffusion system of equations of Gause–Lotka–Volterra type, as a macroscopic model. I explain earlier studies of the two species competition-diffusion system for two native species in the absence of one exotic species. Especially, I explain the asymptotic behaviors of solutions and traveling wave solutions of the system. Next, I introduce the known results on the three species competition-diffusion system which studied the influence of the invasion of one exotic species on two native ones. In addition, I explain the meaning of "weakness" of the exotic species compared with the native ones.

In Chapter 3, I numerically show the behaviors of solutions of the model where one of the coefficients in the system is used as a free parameter and investigate whether or not the invasion of one exotic species influences two native competing species. The numerical result reveals that the resulting behavior is very sensitive to a suitable parameter in a sense that three different types of asymptotic behaviors arise depending on the parameter as follows: (a) the exotic species fades out, but the competitive relation of native species is reversed so that the stronger native species can not survive, (b1) the exotic species survives, so that competitor–mediated coexistence exhibiting complex spatio-temporal pattern occurs, (b2) the exotic species survives, so that competitor–mediated coexistence exhibiting steadily rotating spirals occurs.

In Chapter 4, I introduce the existence of two species- and three species- traveling wave solutions which were obtained in the earlier study on three species competition-diffusion systems. In addition, I briefly mention the planar stability of these traveling wave solutions in two dimensions.

In Chapter 5, I numerically discuss the interaction of two and three species traveling wave solutions in two dimensions and find three types of asymptotic behaviors of solutions which are qualitatively similar to the ones shown in Chapter

3.

In Chapter 6, I investigate the interaction between two and three species traveling wave solutions in one dimension. I observe that the interaction between these traveling wave solutions can be classified into three types, depending on the parameter: (a) collision and reflection, (b) collision and fusion, (c) collision and annihilation. In addition, I show that the three types of asymptotic behaviors in two dimensions can be explained by the interactions between the two and three species traveling waves.

In Chapter 7, I numerically investigate the steadily rotating spirals shown in Chapter 6. I observe that the front and back faces of the spiral arm near the core consist of the two species- and three species- traveling wave solutions, respectively, and the front face approches to the back one of former spiral arm, and homoclinic traveling wave appears. In addition, I discuss the parameter dependency of core radius on the resulting steadily rotating spirals.

In Chapter 8, I discuss about a newly-discovered two dimensional traveling wave solutions which I call *wedge–shaped traveling wave solutions.* Such traveling wave solutions are found in some parameter region where the exotic species can not survive. I explain that this wedge–shaped traveling wave solutions can be understood by suitably-angled superposition of two species- and three species- one dimensional traveling wave solutions. In addition, I show the quantitative relation between the velocities of the two one dimensional traveling wave solutions and the wedge–shaped traveling wave solution.

In Chapter 9, I summarize this thesis. I emphasize that the behavior arising in a three species competition-diffusion system is so sensitive to values of some parameter in the system. Unfortunately, I have not yet fully understood this sensitiveness, although it is caused by the following three factors: (i) planar stability of the two species- and three species- traveling wave solutions, (ii) interaction between the two species- and three species- traveling wave solutions, (iii) difference of speeds of the two species- and three species- traveling wave solutions. In addition, I briefly mention my results from viewpoint of ecology.

Finally, in Appendix, I show the proof of Proposition used in Chapter 8.

Acknowledgments

Special thanks are due to my supervisor Professor Masayasu Mimura for his invaluable support and guidance for the past three decades in particular for his impressible encouragement in the hard moments of graduate school.

I am also grateful to my thesis team fellows: Professor Daishin Ueyama and Professor Yuichiro Wakano for their support, valuable feedback, and insightful ideas to this research.

A part of this thesis was supported by the Meiji University Global COE Program "Formation and Development of Mathematical Sciences Based on Modeling and Analysis."

Finally, I am grateful to Fumiko, My wife and Hatsuho and Manami, My daughters for their warm encouragement.

Contents

List of Figures

Chapter 1

Introduction

With the increasing deterioration of the global environment and the resulting loss of species diversity, research on species diversity is increasingly gaining importance. A good starting point of theoretical research on the issue of species diversity is the law of competitive exclusion, which was proposed by the Russian ecologist, G. Gause [10] who performed experimental studies on two competing species of Paramecium, *P. aurelia* and *P. caudatum*. The law of competitive exclusion can be summarized as follows: "Two species strongly competing for the same resources cannot coexist if other ecological factors are constant." The theoretical basis for conceptualizing this law quantitatively are typically formed using the Lotka–Volterra ordinary differential equations for two competing species:

$$\begin{cases} \frac{du}{dt} = (r_1 - a_1 u - b_{12} v)u, \\ \frac{dv}{dt} = (r_2 - b_{21} u - a_2 v)v. \end{cases} \quad t > 0, \tag{1.1}$$

In (1.1), $u(t)$ and $v(t)$ denote the population densities of two competing species U and V at time t, respectively. The parameters r_i, a_i and b_{ij} $(i, j = 1, 2(i \neq j))$ represent the intrinsic growth rates, intraspecific and interspecific competition rates, respectively, which are all positive constants. The equations given in (1.1) represent a well known fundamental model in mathematical ecology. For this model, strongly competing species U and V can be represented by the following relationship:

$$\frac{a_1}{b_{12}} < \frac{r_1}{r_2} < \frac{b_{21}}{a_2}. \tag{1.2}$$

Under these conditions, any non-negative solution of (1.1) generally tends either to $(r_1/a_1, 0)$ or to $(0, r_2/a_2)$. This means that competitive exclusion occurs between

the two species.

However, strongly competing species exist in nature. To understand why such coexistence appears, many theoretical studies have been performed in the filed of mathematical ecology.

For example, some studies have been undertaken to explore the phenomenon of coexistence resulting from spatial segregation. In this approach, a diffusion term exhibiting the random walk is introduced into the Lotka–Volterra ordinary differential equations (1.1) as follows:

$$\begin{cases} u_t = d_1 \Delta u + (r_1 - a_1 u - b_{12} v)u, \\ v_t = d_2 \Delta v + (r_2 - b_{21} u - a_2 v)v, \end{cases} \quad t > 0, x \in \Omega, \tag{1.3}$$

where the parameters d_1 and d_2 represent diffusion rates, which are positive constants. Let Ω ($\subset \mathbb{R}^M (M = 1, 2)$) be a bounded domain and consider (1.3) in Ω with Neumann boundary conditions:

$$\frac{\partial u}{\partial \nu} = \frac{\partial v}{\partial \nu} = 0, \quad t > 0, x \in \partial\Omega. \tag{1.4}$$

We first note that the stable attractor of (1.3) consists only of equilibrium solutions (Hirsch [12]). On one hand, Kishimoto and Weinberger [21] showed that if Ω is convex, any nonconstant equilibrium solutions are unstable, even if they exist. This means that if (1.3) is satisfied, U and V cannot coexist, no matter if a diffusion effect is introduced. On the other hand, if the domain Ω is not convex, then the structure of equilibrium solutions is not so simple but depends on the shape of Ω. For example, Matano and Mimura [25] showed that if Ω takes a suitable dumbbell shape, then there exist stable non-constant equilibrium solutions that exhibit spatial segregation of the competing species in the sense that one region is nearly occupied by U while the other is occupied by V.

Another way by which strongly competing species U and V might coexist results from the effects of the two species avoiding other species. Shigesada, Kawasaki, and Teramoto [31] proposed the following cross–diffusion equations:

$$\begin{cases} u_t = \Delta \{(d_1 + \alpha_{11} u + \alpha_{12} v)u\} + (r_1 - a_1 u - b_{12} v)u, \\ v_t = \Delta \{(d_2 + \alpha_{21} u + \alpha_{22} v)v\} + (r_2 - b_{21} u - a_2 v)v, \end{cases} \quad t > 0, x \in \Omega, \tag{1.5}$$

where the non-negative parameters $\alpha_{ii}(i = 1, 2)$ and $\alpha_{ij}(i, j = 1, 2(i \neq j))$ represent environmental pressures owing to the intraspecies and interspecies interferences, respectively. Using local bifurcation theory, Mimura and Kawasaki [28] showed that, with boundary conditions (1.4), (1.5) has stable nonconstant equilibrium solutions for a one dimensional problem. Moreover, using singular perturbation methods, Mimura [27] and Mimura, Nishiura, Tesei, and Tsujikawa [29] showed the existence of nonconstant equilibrium solutions, and Kan-non [18] discussed the stability of those solutions.

Another approach exploits the possibility of coexistence when the environment changes in time. In this direction, Hutchinson [15] introduced seasonal effects into the coefficents of the following Lotka–Volterra ordinary differential equations with time dependent coefficients:

$$\begin{cases} u_t = (r_1(t) - a_1(t)u - b_{12}(t)v)u, \\ v_t = (r_2(t) - b_{21}(t)u - a_2(t)v)v, \end{cases} \quad t > 0, \tag{1.6}$$

where $a_i(t)$ and $b_{ij}(t)$ $(i, j = 1, 2 \quad (i \neq j))$ are periodic functions that represent seasonal effects. Cushing [5], Mottoni and Schiaffino [6] showed that (1.6) has stable periodic coexistence solutions.

Similarly, the possibility of coexistence can be considered when the environment changes in space. For example, by using two timing methods, Ei and Mimura [9] discussed how spatial inhomogeneities in the environment can influence the coexistence of two competing species.

In addition, theoretical studies have been conducted on competitor-mediated coexistence in which the number of species is increased, by using the N-species Lotka–Volterra ordinary differential equations:

$$\frac{du_i}{dt} = (r_i - a_i u_i - \sum_{j=1,\cdots,N}^{i \neq j} b_{ij} u_j)u_i, \quad t > 0, \quad (i = 1, \cdots N). \tag{1.7}$$

This approach is based on the idea that "the enemy of my enemy is my friend;" In (1.7), $u_i(t)$ denotes the population density of the i-th species, and r_i, a_i, and b_{ij} $(i, j = 1, 2, \ldots N(i \neq j))$ represent the intrinsic growth rates, intraspecific and interspecific competition rates, respectively. All these parameters are positive constants.

May and Leonard [26] showed the existence of coexistence solutions with non-periodic oscillations in (1.7) with $N = 3$, and Arneodo, Coullet, and Tresser [1] showed the existence of coexistence solutions with chaotic behavior in (1.7) with $N = 4$. One of the important results of this approach is the theorem by Hirsh [13], which asserts that "all of the dynamics of the attractor of N-species competitive Lotka–Volterra ordinary differential equations occur on a manifold of dimension $N-1$." Hirsh's theorem implies that limit cycles cannot exist in (1.7) with $N < 3$, and chaos cannot exist in (1.7) with $N < 4$. Focusing upon (1.7) with $N = 3$, the asymptotic state is either a critical point, a heteroclinic orbit, a combination of heteroclinic orbits, or a limit cycle. The occurrence of the first three can be easily determined from a geometric analysis of nullclines, but the existence of a limit cycle is difficult to be determined. The following question arrises: In which situation would limit cycles exist? Using a geometric analysis of nullclines, Zeeman [34] classified (1.7) with $N = 3$ into 33 possibilities, and van den Driessche and Zeeman [33] showed that 27 of those classes cannot have limit cycles. In the remaining six classes, multiple limit cycles were found one after the other ([14], [23], [24], [11], [22]), but there is yet no complete classification theory that predicts the long-term behavior of these classes.

Recently, the N-species Lotka–Volterra reaction-diffusion equations,

$$\frac{\partial u_i}{\partial t} = d_i \Delta u_i + (r_i - a_i u_i - \sum_{j=1,\cdots,N}^{i \neq j} b_{ij} u_j) u_i, \quad t > 0, x \in \Omega, \quad (i = 1, \cdots N) \quad (1.8)$$

have been studied. Here, d_i is the diffusion rate of population densities u_i $(i = 1, 2, \ldots N)$. Ei, Ikota, and Mimura [8] have shown that (1.8) with $N = 3$ have spatiotemporal inhomogeneous solutions when the species are equivalently strong and involve a cyclic property in some sense. These solutions occur even if the diffusionless system (1.7) has no stable coexistence solutions (as is examined in Chapter 2). Quite recently Chen, Hung, Mimura, Tohma and Ueyama [2] showed the existence of spatial inhomogeneous equilibrium solutions for (1.8) with $N = 3$, even if only one species is the strongest (This is also examined in Chapter 2).

From the viewpoint of competitor-mediated coexistence, it is important to study the influence of exotic species on other native ones as exogenous effect. In

general, exotic species is weaker than the native ones because it has evolved in a different ecological environment ([17]). But even if exotic species is weaker, it might cooperate with weaker native species, after which the cooperation might reverse competitive relations among native species.

From this perspective, the following question is to be addressed: First, consider the situation in which there is a two native species system, where one is stronger than the other in competition, that is, competitive exclusion occurs between them. Second, consider a situation in which a single exotic competing species invades the native system. Is it possible for the modified system of two native species and one exotic species to coexist, even if the exotic species is relatively weaker than either of the native species? In other words, does competitor-mediated coexistence occur by the balance of these three species even if the corresponding equation (1.7) has no stable coexistence solution?

This thesis aims to examine this question from standpoint of (1.8) with $N = 3$.

The content of this thesis is as follows: In Chapter 2, I describe the system which I will use as a model and its underlying assumptions. In Chapter 3, I examine (1.8) with $N = 3$ numerically in a square domain with the Neumann boundary conditions. By taking b_{23} as a free parameter and fixing other parameters suitably, it will be considered whether or not the invasion of an exotic species (say,W) influences the competition of two native species (say, U and V) in the (U, V, W) system. In Chapter 4, I consider three species traveling wave solutions for U, V, and W in order to obtain essential information on the occurrence or nonoccurrence of competitor-mediated coexistence of U, V, and W. In Chapter 5, I evaluate the interaction of two– and three– species traveling wave solutions in two dimensions and show the occurrence of dynamic coexistence of U, V, and W for suitable values of b_{23}. In Chapter 6, to understand the occurrence and nonoccurrence of dynamic coexistence of U, V, and W in two dimensions, I discuss the interactions of two- and three-species traveling wave solutions in one dimension. In Chapter 7, I examine the spiral coexistence of U, V, and W which exhibits dynamic coexistence of the three species and the dependence of the core radius on the parameter b_{23}. In Chapter 8, I discuss the existence of wedge-like traveling wave solutions in two

dimensions. In Chapter 9, I provide concluding remarks on the results obtained in the previous chapters. Finally in Appendix, I prove a proposition used in Chapter 8.

Chapter 2

Model system and assumptions

As a simple situation of competitor-mediated coexistence in spatio-temporally homogeneous environment, I consider the interaction of three competing species under the situation where one exotic competing species (say, W) moving randomly invades system of two native species (say, U and V) which are strongly competing and moving randomly. The situation can be theoretically discussed by the following three-species reaction-diffusion system of Gause–Lotka–Volterra type:

$$\begin{cases} u_t = d_1\Delta u + (r_1 - a_1u - b_{12}v - b_{13}w)u, \\ v_t = d_2\Delta v + (r_2 - b_{21}u - a_2v - b_{23}w)v, \\ w_t = d_3\Delta w + (r_3 - b_{31}u - b_{32}v - a_3w)w, \end{cases} \tag{2.1}$$

where $u(t,x)$, $v(t,x)$ and $w(t,x)$ denote the population densities of U, V and W at time t and position x, respectively. The parameters d_i, r_i, a_i and b_{ij} $(i,j = 1,2,3(i \neq j))$ represent the diffusion rates, intrinsic growth rates, intra-specific and inter-specific competition rates, respectively, which are all positive constants. I consider (2.1) in a bounded domain Ω in $\mathbb{R}^N(N = 1,2)$ where the boundary conditions are

$$\frac{\partial u}{\partial \nu} = \frac{\partial v}{\partial \nu} = \frac{\partial w}{\partial \nu} = 0, \quad t > 0, x \in \partial\Omega, \tag{2.2}$$

where ν is the outerward unit normal vector on the boundary $\partial\Omega$ of Ω and the initial conditions are

$$u(0,x) = u_0(x) \geq 0, \quad v(0,x) = v_0(x) \geq 0, \quad w(0) = w_0(x) \geq 0, \quad x \in \Omega. \tag{2.3}$$

I start with a simple two competing species system of (2.1) in the absense of w,

$$\begin{cases} u_t = d_1 \Delta u + (r_1 - a_1 u - b_{12} v)u, \\ v_t = d_2 \Delta v + (r_2 - b_{21} u - a_2 v)v, \end{cases} \quad t > 0, x \in \Omega \tag{2.4}$$

with the boundary and initial conditions

$$\frac{\partial u}{\partial \nu} = \frac{\partial v}{\partial \nu} = 0, \quad t > 0, x \in \partial\Omega \tag{2.5}$$

and

$$u(0,x) = u_0(x) \geq 0, \qquad v(0,x) = v_0(x) \geq 0, \quad x \in \Omega, \tag{2.6}$$

respectively.

I first note the following two theorems:

Theorem 2.1 (Hirsch [12]). *The stable attractor of* (2.4) - (2.6) *consists of equilibrium solutions.*

Theorem 2.2 (Kishimoto–Weinberger [21]). *If* Ω *is convex, any non-constant equilibrium solutions of* (2.4) - (2.6) *are unstable, even if they exist.*

These theorems indicate that the stable equilibrium solutions of (2.4) without diffusion

$$\begin{cases} \frac{du}{dt} = (r_1 - a_1 u - b_{12} v - b_{13} w)u, \\ \frac{dv}{dt} = (r_2 - b_{21} u - a_2 v - b_{23} w)v, \end{cases} \quad t > 0, \tag{2.7}$$

give an important information on the asymptotic behavior of $(u(t,x), v(t,x))$ of the problem (2.4) – (2.6).

I now impose the following assumption on (2.4):

(A1) $$\frac{a_1}{b_{12}} < \frac{r_1}{r_2} < \frac{b_{21}}{a_2}. \tag{2.8}$$

Then, one finds that stable equilibria of (2.4) and (2.5) are only $(r_1/a_1, 0)$ and $(0, r_2/a_2)$ and moreover, any positive solutions $(u(t,x), v(t,x))$ generically tends to either $(r_1/a_1, 0)$ or $(0, r_2/a_2)$ as t tends to infinity. This ecologically implies that competitive exclusion occurs between U and V as shown in Figure 2.1.

These results give a naive question to the problem (2.4)–(2.6): Which species becomes dominant under strong competition?

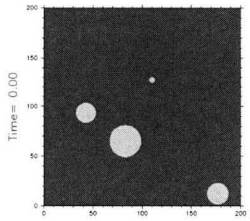

(a1) $t = 0$

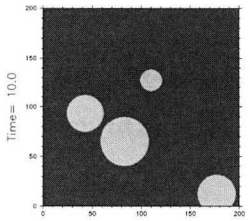

(a2) $t = 3$

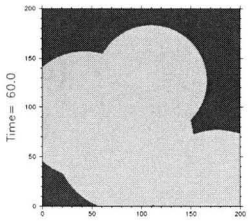

(a3) $t = 20$

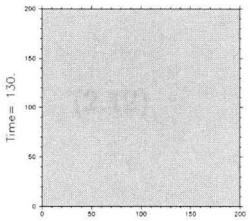

(a4) $t = 50$

(a) U is dominant where $d_i = a_i = 1 (i = 1, 2)$, $r_1 = 28$, $b_{12} = 22/21$, $b_{21} = 37/21$.

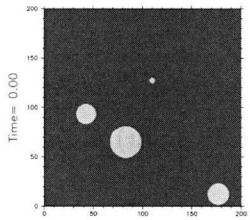

(b1) $t = 0$

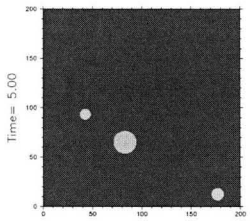

(b2) $t = 2$

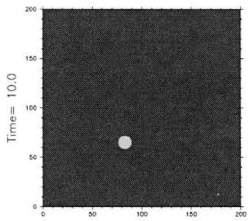

(b3) $t = 3$

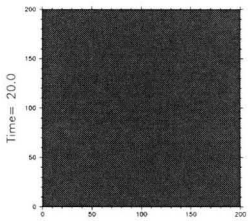

(b4) $t = 10$

(b) V is dominant where $d_i = a_i = 1$ $(i = 1, 2)$, $r_1 = 28$, $b_{12} = 37/21$, $b_{21} = 22/21$.

Figure 2.1: Numerical simulations of (2.4) – (2.6) in $\Omega = (0, 200) \times (0, 200)$ where light and dark gray colors show the areas occupied by U and V, respectively.

In general, this question is difficult to answer. However, one information to answer it is the existence of one dimensional traveling wave solution $(u(z), v(z))(z = x - \theta t)$ with velocity θ. This solution is given by

$$\begin{cases} -\theta u_z = d_1 u_{zz} + (r_1 - a_1\, u - b_{12}\, v)\, u, \\ -\theta v_z = d_2 v_{zz} + (r_2 - b_{21}\, u - a_2\, v)\, v, \end{cases} \quad z \in \mathbb{R}, \tag{2.9}$$

with the boundary conditions

$$\begin{cases} \lim\limits_{z \to -\infty} (u(z), v(z)) = (0, r_2/a_2), \\ \lim\limits_{z \to \infty} (u(z), v(z)) = (r_1/a_1, 0). \end{cases} \tag{2.10}$$

By using a suitable transformation, (2.9) and (2.10) can be rewritten as

$$\begin{cases} -\theta u_z = u_{zz} + (1 - u - cv)\, u, \\ -\theta v_z = d v_{zz} + (a - bu - v)\, v, \end{cases} \quad z \in \mathbb{R}, \tag{2.11}$$

with the boundary conditions

$$\begin{cases} \lim_{z\to-\infty}(u(z),v(z)) = (0,a), \\ \lim_{z\to\infty}(u(z),v(z)) = (1,0). \end{cases} \tag{2.12}$$

Then $(A1)$ is rewritten as

$$\frac{1}{c} < a < b. \tag{2.13}$$

As for traveling wave solutions of (2.11) with (2.13) and (2.12), the following theorems are already known:

Theorem 2.3 (Kan-non [19]). *Under* (2.13), *there is a unique* $\theta = \theta_{uv}$ *such that a solution* $(u(z), v(z))$ *of* (2.11) *and* (2.12) *exists.*

Theorem 2.4 (Kan-non and Fang [20]). *Under* (2.13), *the traveling wave solution* $(u(z), v(z))$ *of* (2.11) *and* (2.12) *is asymptotically stable.*

Theorem 2.5 (Mimura and Rodrigo [30]). *Under* (2.13), *the unique traveling wave solutions* $(u(z), v(z))$ *of* (2.11) *and* (2.12) *can be explicitly represented for suitable parameter regimes of* d, a, b, *and* c, *as follows:*

Type-1

$$\begin{cases} u(z) = \frac{1}{2}\left[1 + \tanh(\frac{\sqrt{2ac}}{4}z)\right], \\ v(z) = \frac{a}{2}\left[1 - \tanh(\frac{\sqrt{2ac}}{4}z)\right]^2 \end{cases} \tag{2.14}$$

with

$$\theta = \frac{-2+ac}{\sqrt{2ac}}, \tag{2.15}$$

provided that

$$d = \frac{1}{3c}, b = 2 + \frac{5a}{3} - ac$$

hold.

Type-2

$$\begin{cases} u(z) = \frac{1}{4}\left[1 + \tanh(\frac{\sqrt{1+ac}}{2\sqrt{6}}z)\right]^2, \\ v(z) = \frac{a}{4}\left[1 - \tanh(\frac{\sqrt{1+ac}}{2\sqrt{6}}z)\right]^2 \end{cases} \tag{2.16}$$

with

$$\theta = \frac{-5+ac}{\sqrt{6+6ac}}, \tag{2.17}$$

provided that

$$d = \frac{5 + 6a - ac}{1 + ac}, b = 5 + 5a - ac$$

hold.

Type-3

$$\begin{cases} u(z) = \frac{1}{4}\left[1 + \tanh(\frac{1}{2\sqrt{6}}z)\right]^2, \\ v(z) = \frac{a}{2}\left[1 - \tanh(\frac{1}{2\sqrt{6}}z)\right] \end{cases} \tag{2.18}$$

with

$$\theta = \frac{-5 + 3ac}{\sqrt{6}}, \tag{2.19}$$

provided that

$$d = 5 + 6a - 3ac, b = \frac{5}{3} + 2a - ac$$

hold.

If the velocity $\theta_{uv} < 0$, I can say that the species U is stronger than V in a sense of coupling of diffusion and competition, as shown Figure 2.2 (a), and if $\theta_{uv} > 0$, vice versa, as shown in Figure 2.2 (b).

Hereafter I assume

(A2) $$\theta_{uv} < 0. \tag{2.20}$$

Under the assumptions $(A1)$ and $(A2)$, I consider the situation where an exotic competing species W invades in the (U, V) system, and discuss the possibility of competitor–mediated coexistence of U and V in the presence of W, by using the three species competition–diffusion system (2.1) with (2.2) and (2.3).

For this problem, I should mention the result obtaind by Ei, Ikota and Mimura [8]. They first consider the diffusionless system corresponding to (2.1)

$$\begin{cases} u_t = (r_1 - a_1 u - b_{12} v - b_{13} w)u, \\ v_t = (r_2 - b_{21} u - a_2 v - b_{23} w)v, \quad t > 0, \\ w_t = (r_3 - b_{31} u - b_{32} v - a_3 w)w, \end{cases} \tag{2.21}$$

and assume that

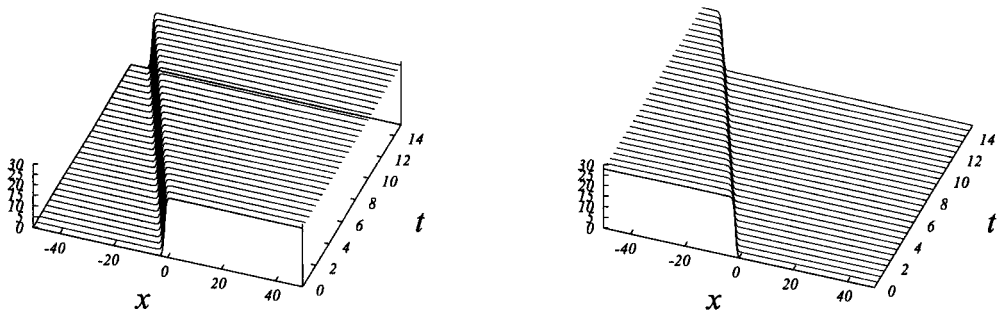

u v

(a) $\theta_{uv} = -2.57\ldots$ where $d_i = a_i = 1 (i = 1, 2)$, $r_1 = 28$, $b_{12} = 22/21$, $b_{21} = 37/21$.

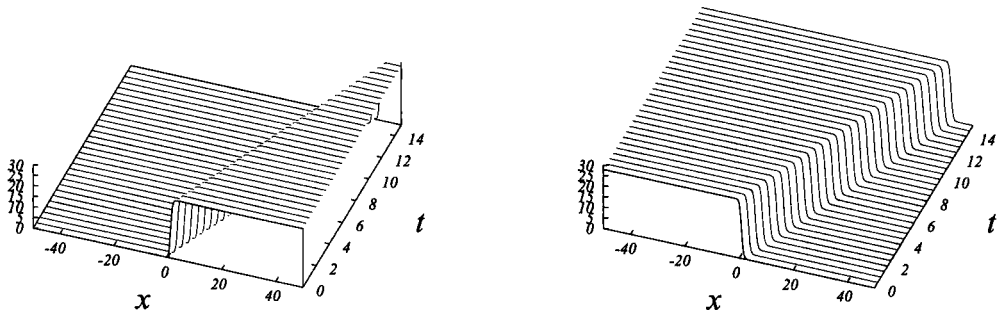

u v

(b) $\theta_{uv} = 2.57\ldots$ where $d_i = a_i = 1 (i = 1, 2)$, $r_1 = 28$, $b_{12} = 37/21$, $b_{21} = 22/21$.

Figure 2.2: Traveling wave solutions of (2.9) and (2.10).

(EIM) $P_1 = (r_1/a_1, 0, 0), P_2 = (0, r_2/a_2, 0)$ and $P_3 = (0, 0, r_3/a_3)$ are asymptotically stable and other critical points are all unstable.

Then it is known that any positive solution of (2.21) generically converges to any one of P_1, P_2 and P_3 ([33]), as shown in Figure 2.3. It ecologically indicates that the exotic species W is strong in the (U, V, W) system in a sense that P_3 is stable. This implies the occurrence of competitive exclusion among U, V and W .

Under this assumption (EIM), if d_1, d_2 and d_3 all sufficiently small, one could expect that the domain Ω is generally divided by U, V and W in a short time as shown in Figure 2.4.

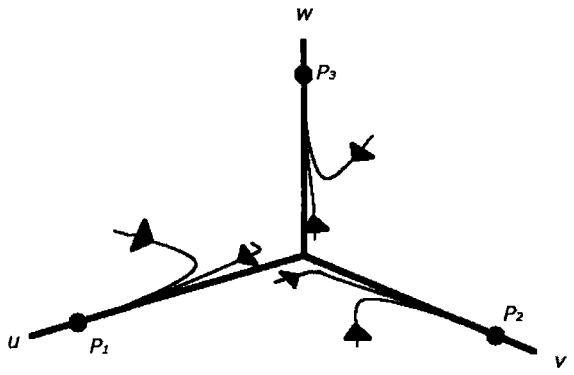

Figure 2.3: Trajectories of (2.21) in (u, v, w)-space where $r_i = a_i = 1$ $(i = 1, 2, 3)$, $b_{12} = b_{23} = b_{31} = 1$, $b_{21} = b_{32} = b_{13} = 3$.

Since stable critical points of (2.21) are only P_1, P_2 and P_3, U and V are strongly competing so that $(A1)$ holds, Therefore, Theorem 2.3 indicate that there is a stable traveling wave solutions $(u(z), v(z))$ $(z = x - \theta_{uv}t)$. Similarly, there are stable traveling wave solutions $(v(z), w(z))$ $(z = x - \theta_{vw}t)$ of

$$\begin{cases} -\theta_{vw}v_z = d_2 v_{zz} + (r_2 - a_2 v - b_{23}w)v, \\ -\theta_{vw}w_z = d_3 w_{zz} + (r_3 - b_{32}v - a_3 w)w, \\ \lim\limits_{z\to-\infty}(v(z), w(z)) = (0, r_3/a_3), \\ \lim\limits_{z\to\infty}(v(z), w(z)) = (r_2/a_2, 0), \end{cases} \quad z \in \mathbb{R}, \tag{2.22}$$

and $(u(z), w(z))$ $(z = x - \theta_{wu}t)$ of

$$\begin{cases} -\theta_{wu}u_z = d_1 u_{zz} + (r_1 - a_1 u - b_{13}w)u, \\ -\theta_{wu}w_z = d_3 w_{zz} + (r_3 - b_{31}u - a_3 w)w, \\ \lim\limits_{z\to-\infty}(u(z), w(z)) = (r_1/a_1, 0), \\ \lim\limits_{z\to\infty}(u(z), w(z)) = (0, r_3/a_3), \end{cases} \quad z \in \mathbb{R}, \tag{2.23}$$

where θ_{vw} and θ_{wu} are the velocities of the traveling wave solutions of (2.22) and (2.23), respectively.

Here, in addition to the assumption (EIM), they assume the parameters d_i, r_i, a_i and $b_{i,j}$ ($i, j = 1, 2, 3 (i \neq j)$) to satisfy

$$\theta_{vw} < 0 \quad \text{and} \quad \theta_{wu} < 0. \tag{2.24}$$

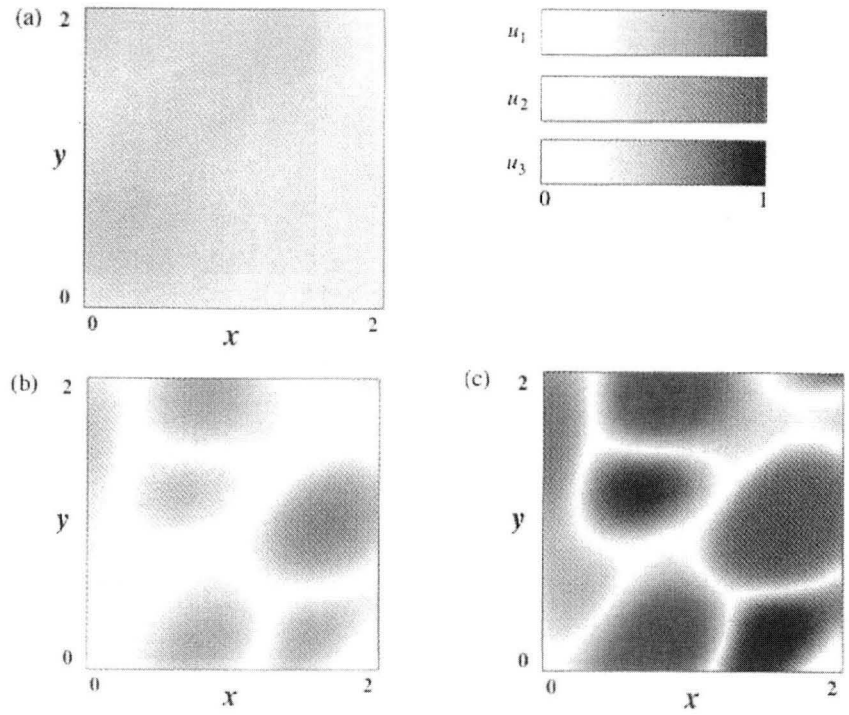

Figure 2.4: Appearance of three phase separation in (2.1)–(2.3) where black, dark gray and light gray colors show the areas occupied by U, V and W, respectively. In addition, it indicates that the darker an area is the more of them are in the area. Furthermore, white colors show the areas not monopolized by a certain species. $d_i = 0.01$, $r_i = a_i = 1$, $b_{ij} = 3$ $(i, j = 1, 2, 3, (i \neq j))$. (a) $t = 0$, (b) $t = 2.5$, (c) $t = 5$. (Figure 1 in [8]).

$(A2)$ and (2.24) indicate that U, V and W possess the cyclic property in a sense of the velocities of traveling wave solutions. Then they demonstrated that spiral-like coexistence of U, V and W occurred, as shown in Figure 2.5.

This result suggests the occurrence of dynamic coexistence among $(u(t,x)$, $v(t,x)$, $w(t,x))$, even if competitive exclusion occurs among $(u(t), v(t), w(t))$ of (2.21). In other words, spatio–temporally inhomogeneous competitor–mediated coexistence occurs, even if it can not appear in the diffusion less system.

I note that in their assumption, the exotic species W is as strong as two native species U and V. But, in general, exotic species are not necessarily stronger and may be weaker than native ones because they have evolved in a different ecological environment ([17]).

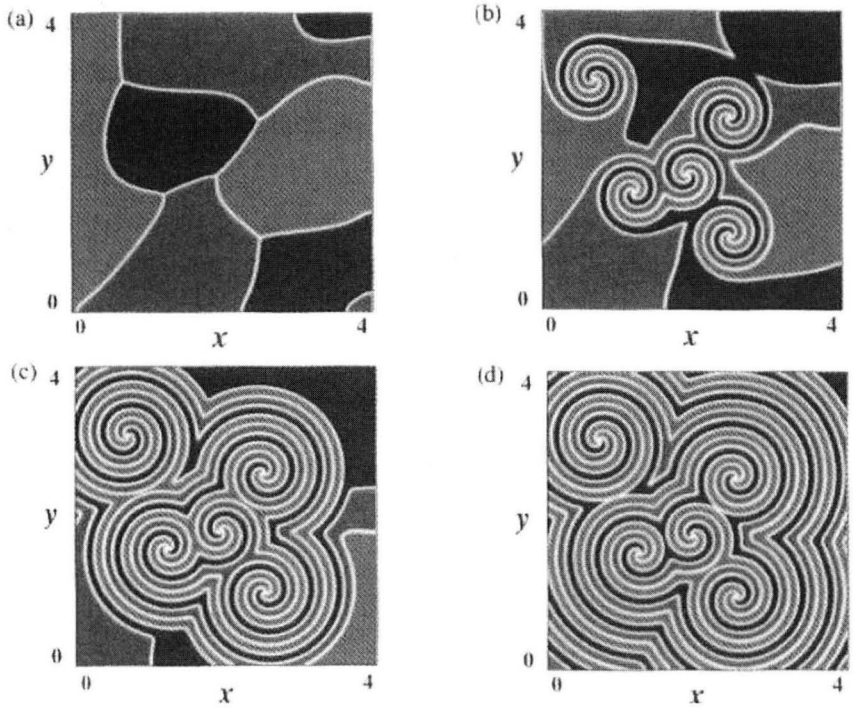

Figure 2.5: Appearance of dynamic spirals of (2.1)–(2.3) where $d_i = 0.01$, $r_i = a_i = 1$, $(i = 1, 2, 3)$, $b_{12} = b_{23} = b_{31} = 2$, $b_{21} = b_{32} = b_{13} = 7$. Black, dark gray and light gray colors show the areas occupied by U, V and W, respectively. Furthermore, white colors show the areas not monopolized by a certain species. (a) $t = 0$, (b) $t = 100$, (c) $t = 200$, (d) $t = 400$. (Figure 4 in [8])

From this reason, I consider the situation that the exotic species W is relatively weak in the (U, V, W) system. Of course, a weak exotic species can not survive in the competing native species, in general. But if the weaker competing native species behave as "the enemy of my enemy is my friend", weaker exotic species may survive. Consequently, the following a naive question arise: can a weaker exotic species change the competitive relation when the weaker native species behave as "the enemy of my enemy is my friend"? Along this direction, I mention the result for (2.1)–(2.3) in [2]. It is assumed that

(CHMTU) For (2.21), $P_1 = (r_1/a_1, 0, 0)$ is stable and a positive critical point $P^* = (u^*, v^*, w^*)$ is also stable, while other critical points including $P_2 = (0, r_2/a_2, 0)$ are all unstable.

This assumption implies that W is weak in sense that $P_3 (= (0, 0, r_3/a_3))$ is unstable. Then it is shown in [2] that there are spatio-inhomogeneous equilibrium solutions exhibiting coexistence of U, V and W, as shown in Figure 2.6.

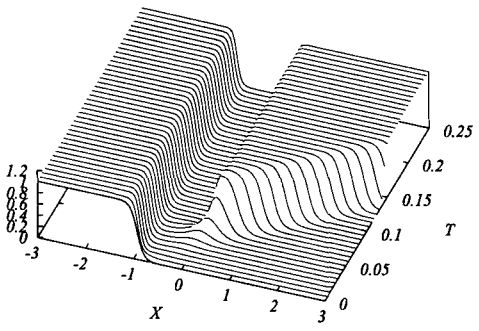

(a) u

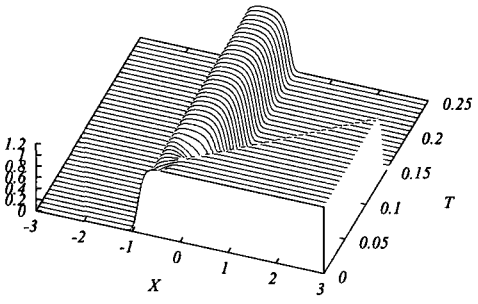

(b) v

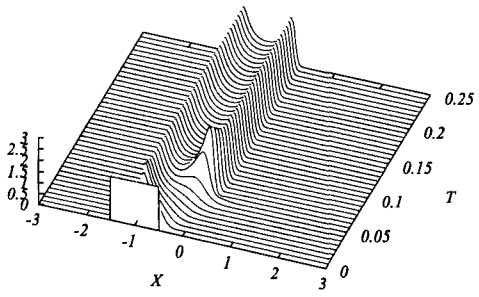

(c) w

Figure 2.6: Numerical simulation of (2.1)–(2.3) where $d_i = 1 (i = 1, 2, 3)$, $r_1 = 576$, $r_2 = \frac{23616}{11}$, $r_3 = \frac{39456}{11}$, $a_1 = 572$, $a_2 = 1804$, $a_3 = 594$,$b_{12} = 308$, $b_{13} = 308$, $b_{21} = 4420$, $b_{23} = 308$, $b_{31} = 5850$, $b_{32} = 2970$ (Figure 9 in [2])

This says that the weak exotic species can change the competitive relation and generates spatially inhomogeneous stable coexistence state. This result seems not to be interesting from the viewpoint of competitor–mediated coexistence, because it already occurs in (2.21), since (u^*, v^*, w^*) is assumed to be stable.

Now, return to the problem stated in Chapter 1: *Is it possible for the modified system of two native species and one exotic species to coexist, even if the exotic species is relatively weaker than either of the native species?* A big difference from

the (EIM) and $(CHMTU)$ is " W is weaker than either of the native species", and this corresponds to $P_1 = (r_1/a_1, 0, 0)$ and $P_2 = (0, r_2/a_2, 0)$ are stable, while $P_3 = (0, 0, r_3/a_3)$ is unstable. More precisely, I assume

(A3) $$\frac{a_2}{b_{32}}, \frac{b_{23}}{a_3} < \frac{r_2}{r_3}, \tag{2.25}$$

which implies that V always survives, while W is always extinct in the absence of U and

(A4) $$\frac{a_3}{b_{13}} < \frac{r_1}{r_3} < \frac{b_{31}}{a_1}, \tag{2.26}$$

which implies that W and U are strongly competing in the absence of V.

Furthermore, I assume

(A5) The positive critical point (u^*, v^*, w^*) of (2.21) does not exist or is unstable even if it exists.

$(A1)$, $(A3)$, $(A4)$ and $(A5)$ indicate that any positive solution $(u(t), v(t), w(t))$ of (2.21) generically tends to either $(r_1/a_1, 0, 0)$ and $(0, r_2/a_2, 0)$ ([3]), that is, the exotic species W does not influence on the (U, V) system so that competitor-mediated coexistence never occurs in (2.21).

Keeping this result in mind, come back to the problem (2.1) – (2.3).

First, I consider the case when $d_i (i = 1, 2, 3)$ are large enough. Then, the following theorem is obtained:

Theorem 2.6 (Conway–Hoff–Smoller [4]). *Suppose that the solutions* $(u(t, x)$, $v(t, x)$, $w(t, x))$ *of* (2.1)–(2.3) *are uniformly bounded in time, Then if* $d_i (i = 1, 2, 3)$ *is large enough,* $(u(t, x), v(t, x), w(t, x))$ *are asymptotically spatially homogeneous.*

However, when all of d_i $(i = 1, 2, 3)$ are not necessarily large, the question whether inhomogeneous asymptotic states exists or not has not been unclear. The aim of this thesis is to answer this question.

First, I note that (2.22) and (2.23) have traveling wave solutions with the velocities θ_{vw} and θ_{wu}, respectively. I should remark that $(A3)$ implies $\theta_{vw} < 0$. As for θ_{wu}, I assume

(A6) $$\theta_{wu} < 0. \tag{2.27}$$

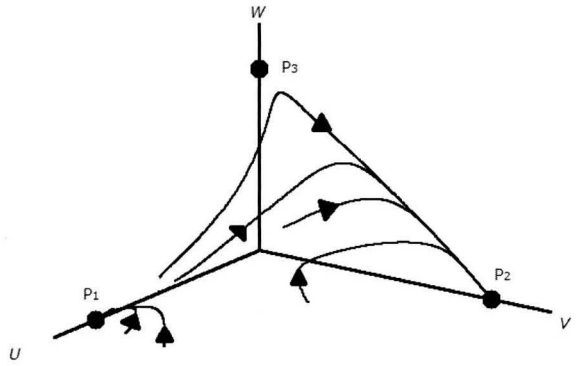

Figure 2.7: Trajectories of solutions of (2.21) in (u, v, w)-space with stable critical point P_1 and P_2 and an unstable critical points P_3 where $r_i = 28$, $a_i = 1$, $b_{12} = 22/21$, $b_{13} = 4$, $b_{21} = 37/21$, $b_{31} = 26/21$, $b_{32} = 22/21$ $(i = 1, 2, 3)$.

Because if $\theta_{wu} > 0$, then by combining with $\theta_{uv} < 0$, one can say that U is stronger than both V and W in the coupling of diffusion and competition. Therefore, competitior–mediated coexistence could not be expected. This is numerically confirmed in Figure 2.8.

Under the assumptions $(A1)$ – $(A6)$, I discuss the problem (2.1)–(2.3) to study the possibility of competitor–mediated coexistence of U and V in the presence of W.

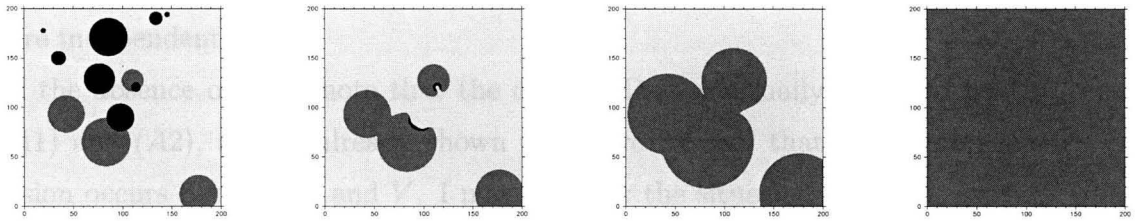

(a1) $t = 0$ (a2) $t = 1$ (a3) $t = 4$ (a4) $t = 20$

Figure 2.8: Numerical simulations of (2.1)–(2.3) for the case $\theta_{wu} > 0$ where $d_1 = 2$, $d_2 = d_3 = 1$, $a_1 = a_2 = 1$, $a_3 = 1.5$, $r_i = 28(i = 1, 2, 3)$, $b_{12} = 22/21, b_{13} = 2, b_{21} = 37/21, b_{23} = 0.75, b_{31} = 26/21, b_{32} = 22/21$. Dark gray, light gray and black colors show the areas occupied by U, V and W, respectively.

Chapter 3

Numerical simulations

In this chapter, I numerically study the two dimensional problem of (2.1)–(2.3), fixing the parameters in (2.1) as

$$d_1 = 1, d_2 = 1, d_3 = 1, \tag{3.1a}$$

$$r_1 = 28, r_2 = 28, r_3 = 28, \tag{3.1b}$$

$$a_1 = 1, a_2 = 1, a_3 = 1, \tag{3.1c}$$

$$b_{12} = 22/21, b_{13} = 4, b_{21} = 37/21, b_{31} = 26/21, b_{32} = 22/21 \tag{3.1d}$$

and taking b_{23} as a free parameter, for which

$$0 < b_{23} < 1 \tag{3.2}$$

is required by $(A2)$. I note that critical points of (2.21) except for the positive one are independent of b_{23}.

In the absence of W, I note that the domain Ω is eventually occupied by U by $(A1)$ and $(A2)$, as was already shown in Figure 2.1 (a), that is, competitive exclusion occurs between U and V. I now consider the situation where an exotic species W invades in the (U, V) system at some time (say, $t = 3.0$), as shown in Figure 2.1 (a2).

When $b_{23} = 0.2$, Figures 3.1 (a) and (b) exhibit that when W invades the V-region in Ω, it immediately fades out, because W is absolutely weaker than V. When W invades vicinities of the boundaries of U– and V–regions, it strongly interacts with U and V so that U, V and W seem to persist for some time. Here

two interesting behaviors can be observed in Figure 3.1: One is the occurrence of a traveling wave like behavior of the three species U, V and W as shown in Figures 3.1 (f) and (g), and the other is the situation where the domain Ω is finally occupied by only V, as shown in Figures 3.1 (f)–(h). These clearly indicate that the cooperation of V and W reverses the competitive relation with U. When $b_{23} = 0.4$, the behavior is drastically changed. Figure 3.2 demonstrates the appearance of complex spatio-temporal coexistence of the three competing species U, V and W. When $b_{23} = 0.6$, as shown in Figure 3.3, one can observe spatial–temporal coexistence, too, but the behavior is different from the previous one in a sense that there successively occur a pair of rotating spirals of the three species. When $b_{23} = 0.8$, as shown in Figure 3.4, the behavior becomes much simpler so that only V survives. Consequently, one can see that competitor-mediated dynamic coexistence occurs between U and V in the presence of W, sensitively depending on values of b_{23}, even if U and V have a relation of competition exclusion in the absence of W and W is weaker than the native species.

In the succeeding chapters, I will discuss why the behavior is so sensitive to values of b_{23}.

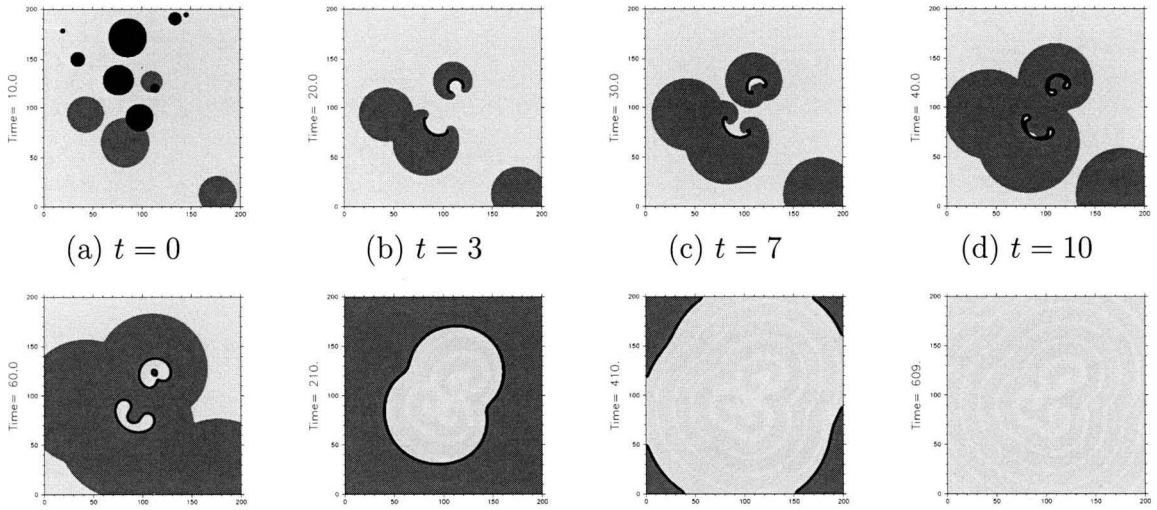

(a) $t = 0$ (b) $t = 3$ (c) $t = 7$ (d) $t = 10$

(e) $t = 18$ (f) $t = 65$ (g) $t = 130$ (h) $t = 200$

Figure 3.1: Invasion of W into (U, V) system where d_i, r_i, a_i and $b_{i,j}(i, j = 1, 2, 3(i \neq j))$ satisfy (3.1) and $b_{23} = 0.2$. Cooperation of V and W reverses the competitive relation with U. Dark gray, light gray, and black colors indicate the areas occupied by U, V and W, respectively.

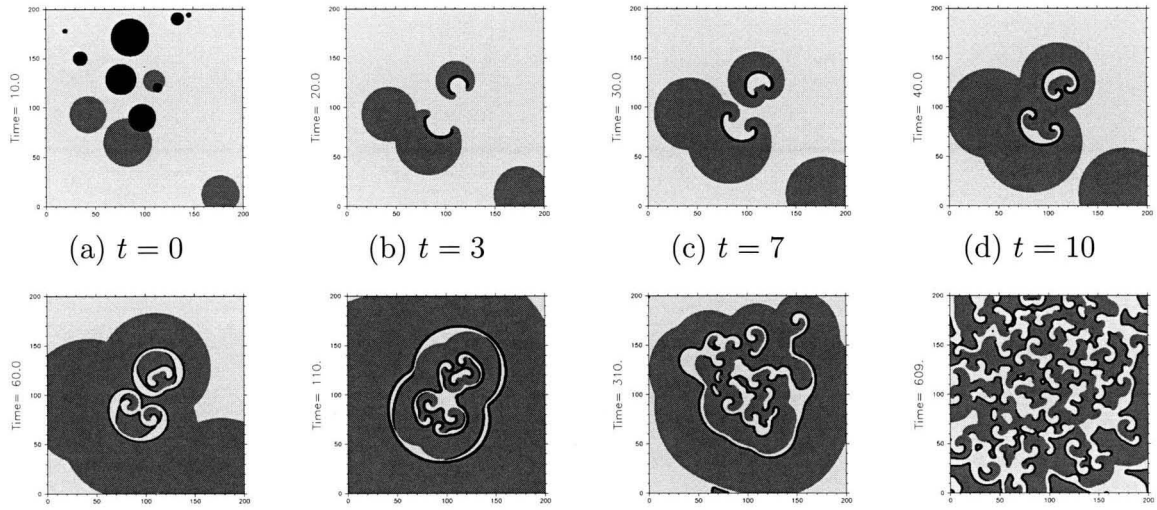

(a) $t = 0$ (b) $t = 3$ (c) $t = 7$ (d) $t = 10$

(e) $t = 18$ (f) $t = 33$ (g) $t = 100$ (h) $t = 200$

Figure 3.2: Invasion of W into (U, V) system where d_i, r_i, a_i and $b_{i,j}(i, j = 1, 2, 3(i \neq j))$ satisfy (3.1) and $b_{23} = 0.4$. Complex spatio–temporal coexistence appears. Dark gray, light gray, and black colors indicate the areas occupied by U, V and W, respectively.

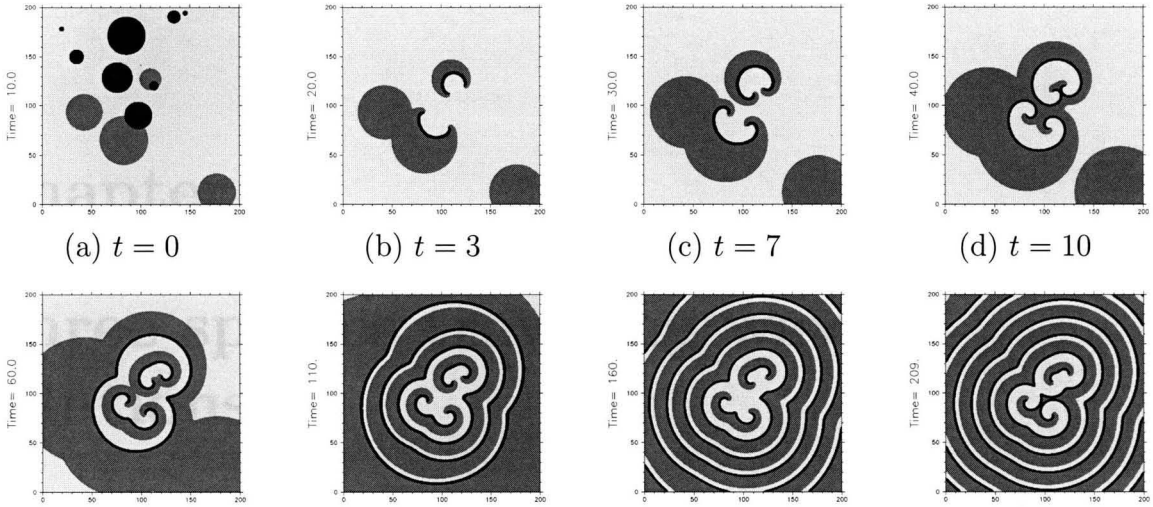

(a) $t = 0$ (b) $t = 3$ (c) $t = 7$ (d) $t = 10$

(e) $t = 18$ (f) $t = 33$ (g) $t = 50$ (h) $t = 65$

Figure 3.3: Invasion of W into (U, V) system where d_i, r_i, a_i and $b_{i,j}(i, j = 1, 2, 3(i \neq j))$ satisfy (3.1) and $b_{23} = 0.6$. Steadily rotating spirals appear. Dark gray, light gray, and black colors indicate the areas occupied by U, V and W, respectively.

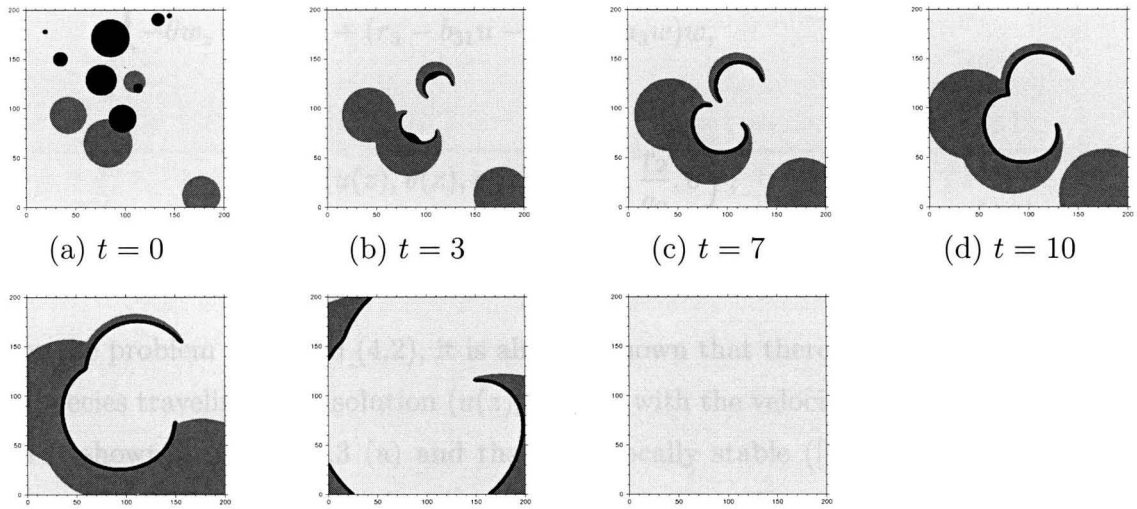

(a) $t = 0$ (b) $t = 3$ (c) $t = 7$ (d) $t = 10$

(e) $t = 18$ (f) $t = 33$ (g) $t = 65$

Figure 3.4: Invasion of W into (U, V) system where d_i, r_i, a_i and $b_{i,j}(i, j = 1, 2, 3(i \neq j))$ satisfy (3.1) and $b_{23} = 0.8$. Cooperation of V and W reverses the competitive relation with U. Dark gray, light gray, and black colors indicate the areas occupied by U, V and W, respectively.

Chapter 4

Three species traveling wave solutions

I first note that Figures 3.1 (f) and (g) suggest the appearance of a three species traveling wave which is represented by a solution of the form $(u(z), v(z), w(z))(z = x - \theta t)$ with velocity θ satisfying

$$\begin{cases} -\theta u_z = d_1 u_{zz} + (r_1 - a_1 u - b_{12} v - b_{13} w)u, \\ -\theta v_z = d_2 v_{zz} + (r_2 - b_{21} u - a_2 v - b_{23} w)v, \\ -\theta w_z = d_3 w_{zz} + (r_3 - b_{31} u - b_{32} v - a_3 w)w, \end{cases} \qquad z \in \mathbb{R}, \tag{4.1}$$

and

$$\begin{cases} \lim_{x \to -\infty} (u(z), v(z), w(z)) = \left(0, \frac{r_2}{a_2}, 0\right), \\ \lim_{x \to \infty} (u(z), v(z), w(z)) = \left(\frac{r_1}{a_1}, 0, 0\right). \end{cases} \tag{4.2}$$

For the problem (4.1) and (4.2), it is already known that there uniquely exists a two species traveling wave solution $(u(z), v(z), 0)$ with the velocity $\theta = \theta_{uv} (< 0)$, which is shown in Figure 4.3 (a) and that it is locally stable ([16]). I call this traveling wave solution a *trivial* one. A natural question arises: do *non-trivial* traveling wave solutions of (4.1) and (4.2) exist? Unfortunately, it has not yet proven. However, recently, for some parameter regime, exact non–trivial traveling wave solutions have been found:

Theorem 4.1 (Chen–Hung–Mimura–Ueyama[3]). *The problem* (4.1) *and* (4.2)

admit an exact traveling wave solution $(u(z), v(z), w(z))$ *of the form*

$$\begin{cases} u(z) = \frac{r_1}{2a_1}(1 + \tanh z), \\ v(z) = \frac{r_2}{4a_2}(1 - \tanh z)^2, \\ w(z) = \frac{4d_1 - 20d_3 - r_1 + r_3}{4(a_3 - b_{13})}(1 + \tanh^2 z), \end{cases} \tag{4.3}$$

with

$$\theta = \frac{4a_3d_1 - 20b_{13}d_3 - a_3r_1 + b_{13}r_3}{2(a_3 - b_{13})}, \tag{4.4}$$

provided that

$$\begin{aligned} b_{12} &= \frac{a_2(8a_3d_1 - 4b_{13}d_1 - 20b_{13}d_3 - b_{13}r_1 + b_{13}r_3)}{(a_3 - b_{13})r_2}, \\ b_{21} &= \frac{a_1(-8a_3d_1 + 16a_3d_2 - 16b_{13}d_2 + 40b_{13}d_3 + 2a_3r_1 + a_3r_2 - b_{13}r_2 - 2b_{13}r_3)}{(a_3 - b_{13})r_1}, \\ b_{23} &= \frac{-24a_3d_2 + 24b_{13}d_2 + a_3r_2 - b_{13}r_2}{4d_1 - 20d_3 - r_1 + r_3}, \\ b_{31} &= \frac{-4a_1a_3d_1 + 4a_1a_3d_3 + 16a_1b_{13}d_3 + a_1a_3r_1 + a_1a_3r_3 - 2a_1b_{13}r_3}{(a_3 - b_{13})r_1}, \\ b_{32} &= \frac{a_2(4a_3d_1 + 4a_3d_3 - 24b_{13}d_3 + a_3r_1 + a_3r_3)}{(a_3 - b_{13})r_2} \end{aligned}$$

hold.

For example, if d_i, r_i, a_i and $b_{i,j}(i, j = 1, 2, 3(i \neq j))$ are specified to satisfy (3.1) and $b_{23} = 3/4$, the exact solution $(u(z), v(z), w(z))$ of (4.1) and (4.2) is explicitly given by

$$\begin{cases} u(z) = 14(1 + \tanh z), \\ v(z) = 7(1 - \tanh z)^2, \\ w(z) = \frac{4}{3}(1 + \tanh^2 z), \\ \theta = -\frac{4}{3}, \end{cases} \tag{4.5}$$

which is shown in Figure 4.1.

By using the numerical method of AUTO ([7]), they drew the global solution structure of non-trivial traveling wave solutions of (4.1) and (4.2) when b_{23} is varied, as shown in Figure 4.3, where the upper solution branch is stable, while the lower one is unstable. When b_{23} takes $0.2, 0.4, 0.6$, and 0.8, for instance, the corresponding velocity θ_{uvw} of the stable non-trivial traveling wave solution is numerically obtained as $\theta_{uvw} = 0.69\ldots, 1.30\ldots, 1.97\ldots$ and $2.92\ldots$, respectively.

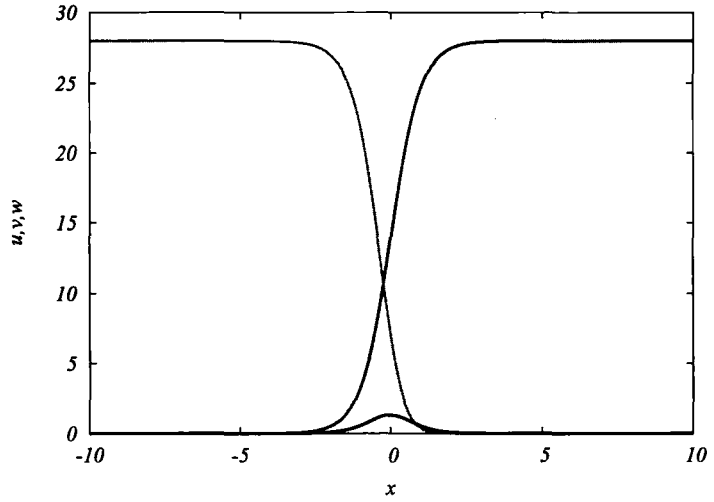

Figure 4.1: An exact solution of (4.1) and (4.2), where d_i, r_i, a_i and $b_{i,j}(i,j = 1,2,3(i \neq j))$ are specified to satisfy (3.1) and $b_{23} = 3/4$. The light gray, dark gray and black lines represent u, v and w, respectively.

For $b_{23} = 0.8$, Figures 4.3 (a), (b) and (c) demonstrate one trivial and stable and unstable non–trivial traveling wave solutions.

I thus find that (4.1) and (4.2) have *two* stable traveling wave solutions. I numerically confirm that these traveling wave solutions are planary stable in two dimensional problem as shown in Figures 4.4 and 4.5.

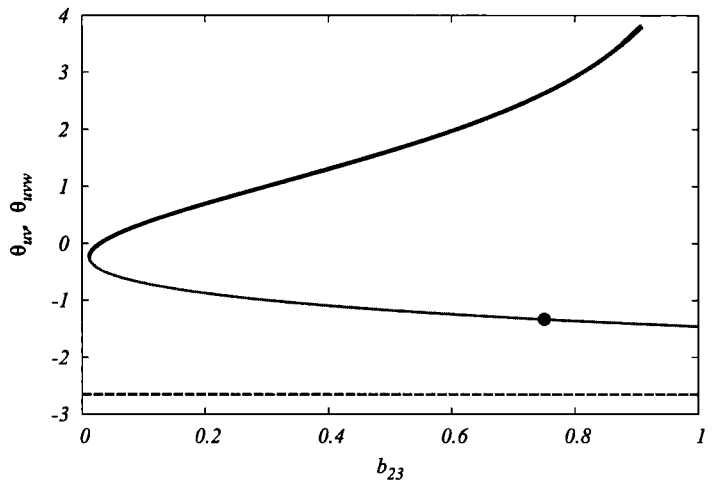

Figure 4.2: Global structure of traveling wave solutions when b_{23} is varied ([3]), where d_i, r_i, a_i and $b_{i,j}(i,j = 1,2,3(i \neq j))$ are specified to satisfy (3.1). Solid black and gray lines represent stable and unstable non-trivial traveling wave solutions, respectively, while the dashed black line represents a stable trivial traveling wave solution, which is independent of b_{23}. A black circle indicates the exact non–trivial traveling wave solution shown in Figure 4.1.

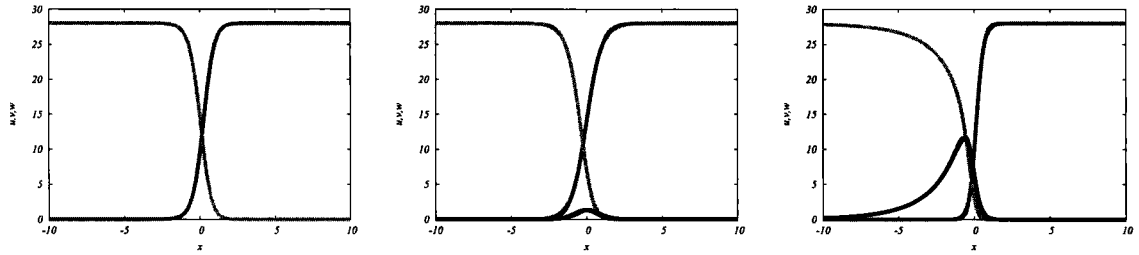

(a) Stable trivial traveling wave . $\theta_{uv} = -2.57\ldots$

(b) Unstable non-trivial traveling wave $\theta_{uvw} = -1.36\ldots$

(c) Stable non-trivial traveling wave $\theta_{uvw} = 2.92\ldots$

Figure 4.3: Trivial and non-trivial traveling wave solutions of (4.1) ([3]), where d_i, r_i, a_i and $b_{i,j}(i,j = 1,2,3(i \neq j))$are specified to satisfy (3.1) and $b_{23} = 0.8$. The light gray, dark gray and black lines represent u, v and w, respectively.

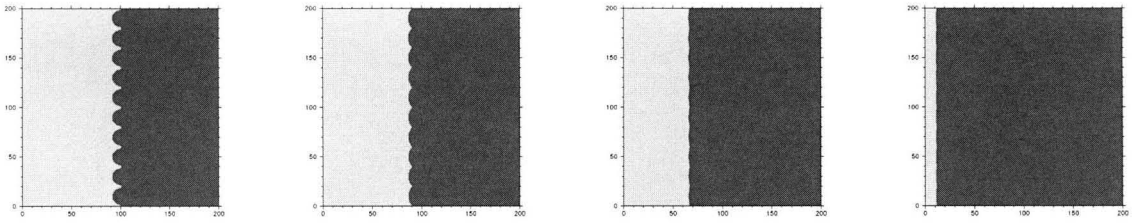

(a) $t = 0$ (b) $t = 2$ (c) $t = 10$ (d) $t = 30$

Figure 4.4: Planar stability of two–species traveling wave solution in Figure 4.3 (a) where d_i, r_i, a_i and $b_{i,j}(i, j = 1, 2, 3(i \neq j))$ are specified to satisfy (3.1) and $b_{23} = 0.80$. Dark gray and light gray indicate the areas occupied by U and V, respectively.

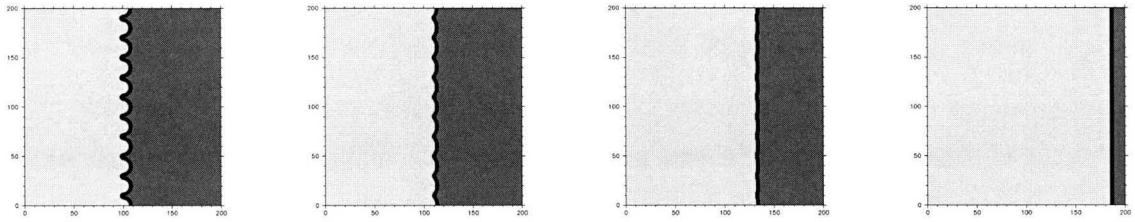

(a) $t = 0$ (b) $t = 2$ (c) $t = 10$ (d) $t = 30$

Figure 4.5: Planar stability of three–species traveling wave solution in Figure 4.3 (c) where d_i, r_i, a_i and $b_{i,j}(i, j = 1, 2, 3(i \neq j))$ are specified to satisfy (3.1) and $b_{23} = 0.80$. Dark gray, light gray, and black colors indicate the areas occupied by U, V and W, respectively.

Chapter 5

Interaction of two species- and three species- traveling waves in two dimensions

In Chapter 4, I numerically showed that there are two stable traveling wave solutions of (4.1) and (4.2), that is, one trivial traveling wave solution which consists of two species and one non–trivial one which consists of three species. In this chapter, I consider the interaction of these two stable traveling waves in a square domain Ω when the initial functions for (2.3) are suitably specified as shown in Figure 5.1. In the upper half region of Ω, I take the stable two species traveling wave solution ($W \equiv 0$) with velocity $\theta_{uv} = -2.57\ldots$ and in the lower half one of Ω, the stable three species traveling wave solution with velocity $\theta_{uvw}(> 0)$, which depends on the value of b_{23}.

When $b_{23} = 0.2$ ($\theta_{uvw} = 0.69\ldots$), as shown in Figures 5.2 (a) – (c), the two species traveling wave begins to move to the left direction in the upper region and conversely, the three species one begins to move to the right direction. In consequence, the area of V is surrounded by the one of U, as shown in Figures 5.2 (c)–(e), After that, the area of V gradually expands and eventually occupies the whole domain Ω, as shown in Figures 5.2 (f)–(h). When $b_{23} = 0.4$ ($\theta_{uvw} = 1.30\ldots$), as is shown in Figure 5.3 (a) – (c), the behavior is quite similar to the case for $b_{23} = 0.2$ (Figure 5.2 (a) – (c)). However, after that, there occurs very irregular complex spatio–temporal pattern which exhibits the dynamic coexistence of U, V and W, as shown in Figure 5.3 (h). When $b_{23} = 0.6$ ($\theta_{uvw} = 1.97\ldots$), as shown in

Figure 5.4, a steadily rotating spiral of U, V and W can be clearly seen. Finally when $b_{23} = 0.8$ ($\theta_{uvw} = 2.92\ldots$), the behavior is so simple and that V eventually occupies the whole domain Ω as shown in Figure 5.5.

The numerical simulations above indicate that either appearance or non-appearance of competitor–mediated coexistence really depends on values of b_{23}.

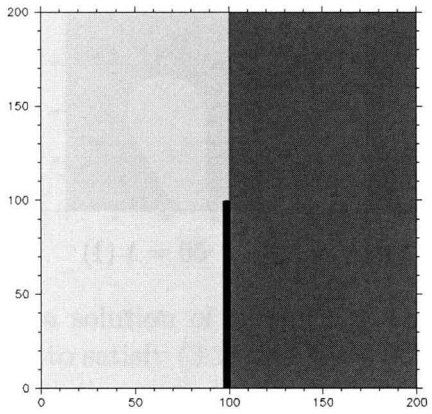

Figure 5.1: Initial profile $(u_0(x,y), v_0(x,y), w_0(x,y))$ of (2.3) in Ω where dark gray, light gray, and black colors indicate the areas occupied by U, V and W, respectively.

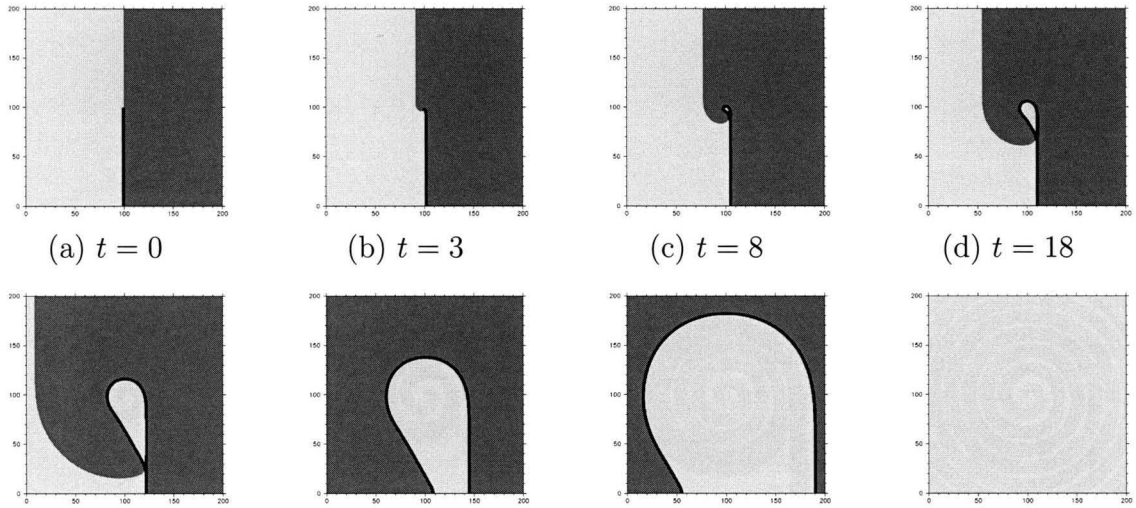

(a) $t = 0$ (b) $t = 3$ (c) $t = 8$ (d) $t = 18$

(e) $t = 33$ (f) $t = 65$ (g) $t = 130$ (h) $t = 218$

Figure 5.2: Dynamics of a solution of (2.1)–(2.3) where d_i, r_i, a_i and $b_{i,j}(i, j = 1, 2, 3(i \neq j))$ are specified to satisfy (3.1) and $b_{23} = 0.2$. Cooperation of V and W reverses the competitive relation with U. Dark gray, light gray, and black colors indicate the areas occupied by U, V and W, respectively.

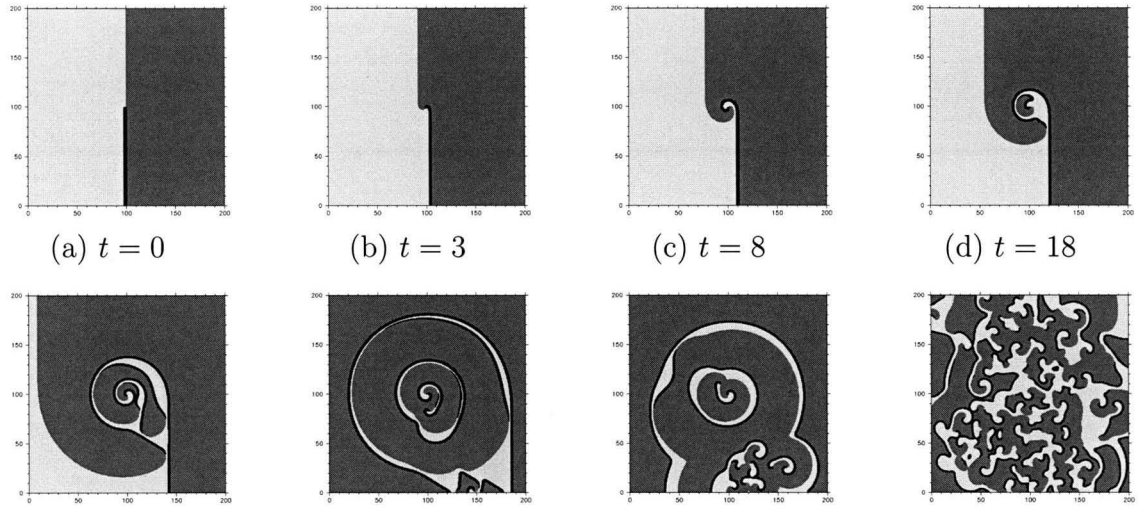

(a) $t = 0$ (b) $t = 3$ (c) $t = 8$ (d) $t = 18$

(e) $t = 33$ (f) $t = 65$ (g) $t = 130$ (h) $t = 250$

Figure 5.3: Dynamics of a solution of (2.1)–(2.3) where d_i, r_i, a_i and $b_{i,j}(i, j = 1, 2, 3(i \neq j))$ are specified to satisfy (3.1) and $b_{23} = 0.4$. Complex spatio–temporal coexistence appears. Dark gray, light gray, and black colors indicate the areas occupied by U, V and W, respectively.

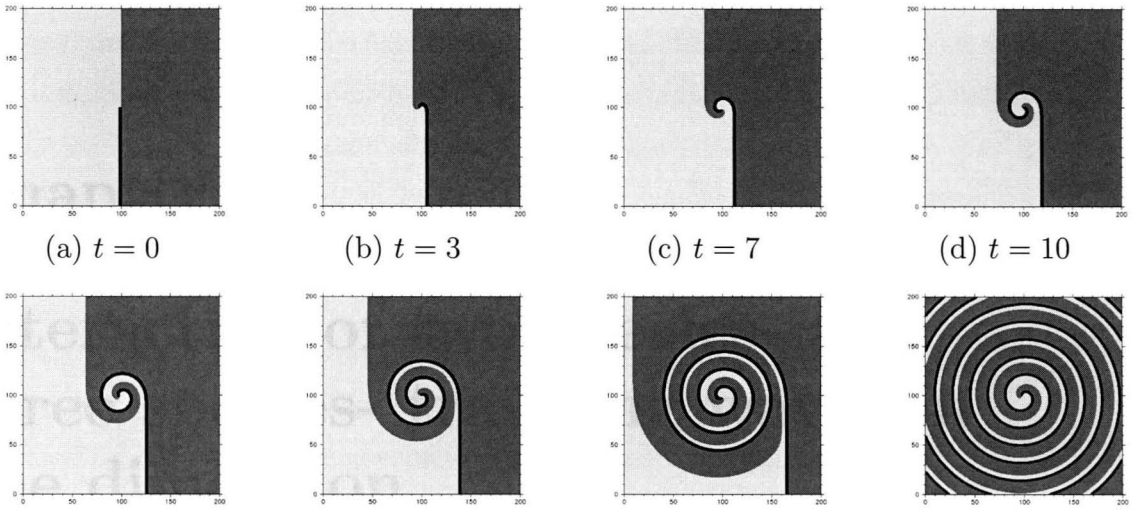

(a) $t = 0$ (b) $t = 3$ (c) $t = 7$ (d) $t = 10$

(e) $t = 14$ (f) $t = 20$ (g) $t = 33$ (h) $t = 65$

Figure 5.4: Dynamics of a solution of (2.1)–(2.3) where d_i, r_i, a_i and $b_{i,j} (i, j = 1, 2, 3 (i \neq j))$ are specified to satisfy (3.1) and $b_{23} = 0.6$. Steadily rotating spirals appear. Dark gray, light gray, and black colors indicate the areas occupied by U, V and W, respectively.

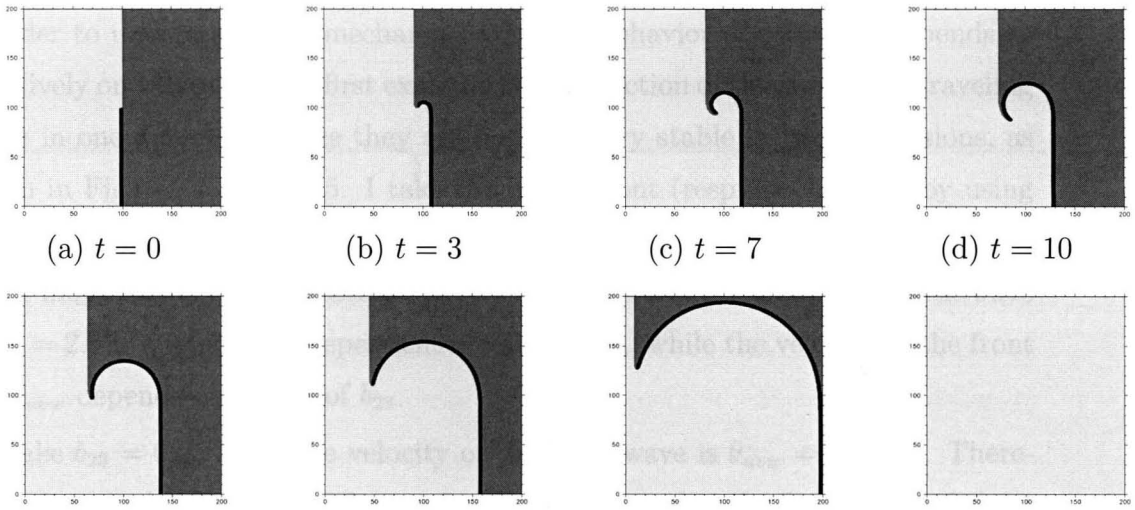

(a) $t = 0$ (b) $t = 3$ (c) $t = 7$ (d) $t = 10$

(e) $t = 14$ (f) $t = 20$ (g) $t = 33$ (h) $t = 57$

Figure 5.5: Dynamics of a solution of (2.1)–(2.3) where d_i, r_i, a_i and $b_{i,j} (i, j = 1, 2, 3 (i \neq j))$ are specified to satisfy (3.1) and $b_{23} = 0.8$. Cooperation of V and W reverses the competitive relation with U. Dark gray, light gray, and black colors indicate the areas occupied by U, V and W, respectively.

Chapter 6

Interaction of two species- and three species- traveling waves in one dimension

In Chapter 5, I considered the interaction of a two species- and three species-traveling wave in two dimensions when b_{23} is varied. When $b_{23} = 0.2$ or 0.8, only V is dominant, that is, competitive exclusion occurs, while when $b_{23} = 0.4$ or 0.6, U, V and W dynamically coexist, that is, competitor-mediated coexistence occurs. In order to understand the mechanism why the behavior of solutions depends so sensitively on values of b_{23}, I first examine the interaction of the two stable traveling waves in one dimension since they are both planary stable in two dimensions, as shown in Figures 4.4 and 4.5. I take the initial front (resp. back) wave by using the three (resp. two) species traveling wave, as shown in Figure 6.1 (a), both of which move to the right direction. Here I note that the velocity of the back wave is $\theta_{uv} = 2.57\ldots$ which is independent of value of b_{23}, while the velocity of the front one θ_{uvw} depends on values of b_{23}.

Take $b_{23} = 0.2$. Then the velocity of the front wave is $\theta_{uvw} = 0.69\ldots$. Therefore, since the back wave which is rather faster approaches the front one and then, instead of colliding, there appears a new three species traveling wave solution which moves to the opposite direction with speed $\theta = -0.69\ldots$, as if it were reflecting, as shown in Figure 6.1. I note that this phenomenon can be observed in the two dimensional behavior as shown in Figures 5.2 (d),(e) and (f). When $b_{23} = 0.4$ ($\theta_{uvw} = 1.30\ldots$), the back wave is still faster than the front one, so

that the behavior after the interaction of the two waves is similar to the one for $b_{23} = 0.2$, as shown in Figures 5.3 (a)–(c). However, after that, the behavior was quite different from the one for $b_{23} = 0.2$. It is rather complex, as exhibited in Figures 5.3 (d)–(h). To examine what happen in Figure 5.3, I show Figure 6.3 for detail between Figure 5.3 (c) and (d), and Figure 6.4 for detail after Figure 5.3 (g). As shown in Figures 6.3 and 6.4, when the three species traveling like wave approaches to the two species one, there appears a new three species traveling like wave which moves to the opposite direction as if it are reflecting, and when the three species ones approaches to each other, they collide and annihilate each other, and then, reflection and annihilation generate complex behavior.

When $b_{23} = 0.6$ ($\theta_{uvw} = 1.97\ldots$), the back wave is slightly faster than the front one, so that a homoclinic type traveling wave appears, as shown in Figure 6.5. This suggests that homoclinic traveling wave solution $(u(z), v(z), w(z))(z = x - \theta t)$ of (4.1) satsfying the boundary conditions

$$\lim_{|z|\to\infty} (u(z), v(z), w(z)) = \left(\frac{r_1}{a_1}, 0, 0\right) \tag{6.1}$$

exists.

By using this homoclinic traveling wave solution, I constract the initial conditions $(u_0(x, y), v_0(x, y), w_0(x, y))$ in square domain Ω in a way that $(r_1/a_1, 0, 0)$ in the upper half region of Ω, and the homoclinic traveling wave solution in the lower one of Ω, as shown in Figure 6.6 (a). Then there appears a steadily rotating spiral pattern as shown in Figure 6.6 (h). Therefore, I could suggest that if a stable homoclinic traveling wave solutions exist in one dimension, a rotating spiral occurs in two dimensions. This scenario is similar to the occurrence of rotating spirals arising in the Belousov-Zhabotinsky reaction ([32]) . Here I also note that this spiral pattern looks almost exactly like the one in Figure 5.4 (h).

On the other hand, when $b_{23} = 0.8$ ($\theta_{uvw} = 2.92\ldots$), oppositely, the front wave is faster than the back one, so that the front wave is gradually leaving from the back one (Figure 6.7).

For the interaction of the two species- and three species- traveling waves in one dimension, I can consider another situation where the back (resp. front) waves are the three–species (resp. two–species) traveling waves, which move to the right

direction, as shown in Figure 6.8 (a). When $b_{23} = 0.2, 0.4$ and 0.6, the front wave is faster than the back one so that the front wave is gradually leaving from the back one (for instance, see Figure 6.8). On the contrary, when $b_{23} = 0.8$, the front wave is slower than the back one so that two waves approach and then annihilate each other in collision (Figure 6.9).

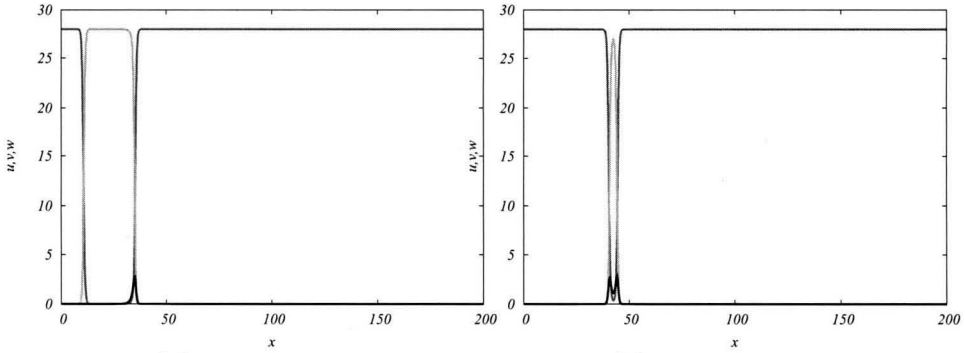

(a) $t = 0$ (b) $t = 14$

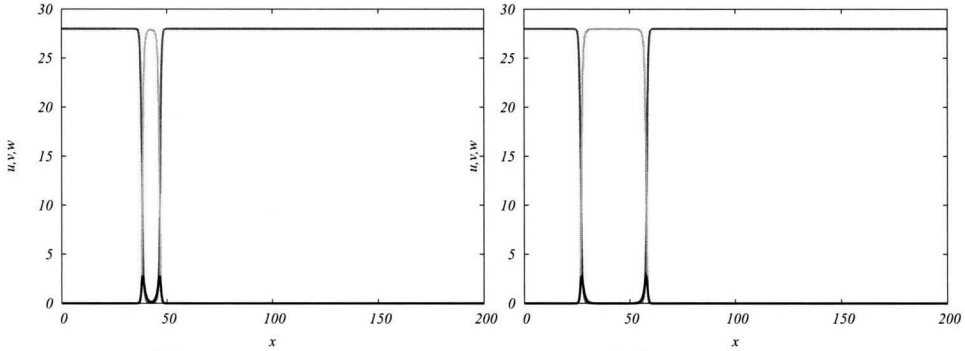

(c) $t = 18$ (d) $t = 33$

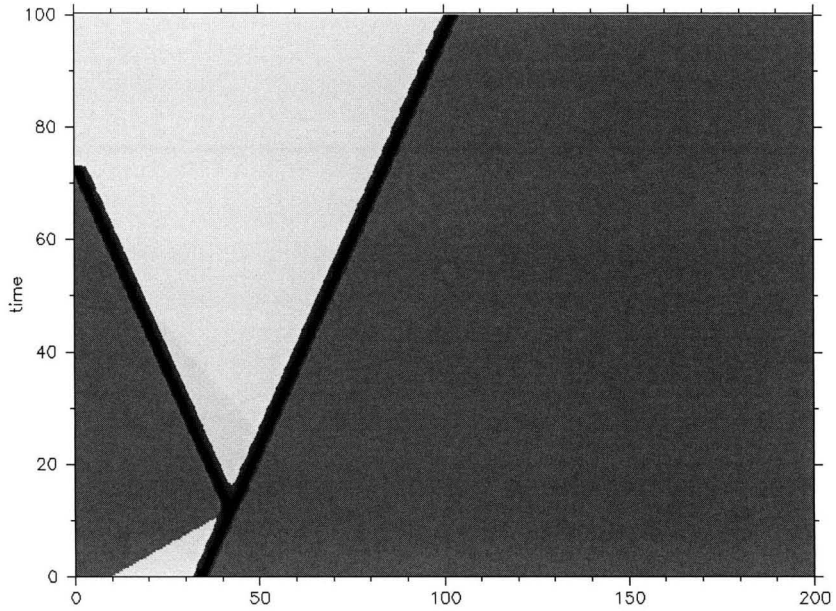

(e)

Figure 6.1: Interaction of two species- and three- species traveling wave solutions of (2.1)–(2.3) in one dimension where the parameters are specified to satisfy (3.1) and $b_{23} = 0.2$. Dark gray, light gray and black colors indicate the areas occupied by U, V and W, respectively.

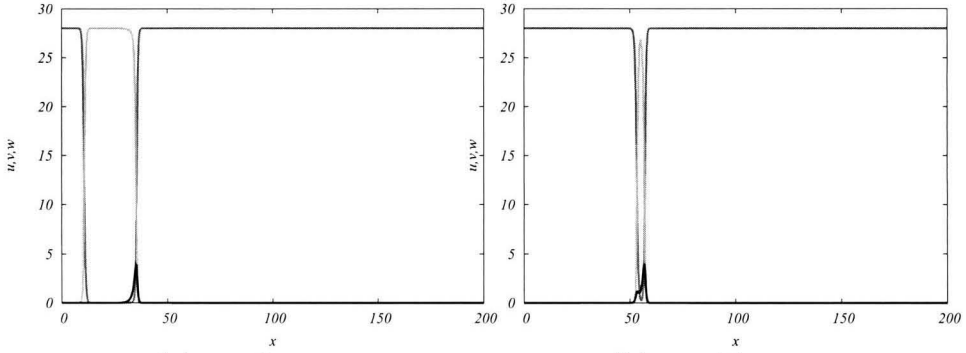

(a) $t = 0$ (b) $t = 18$

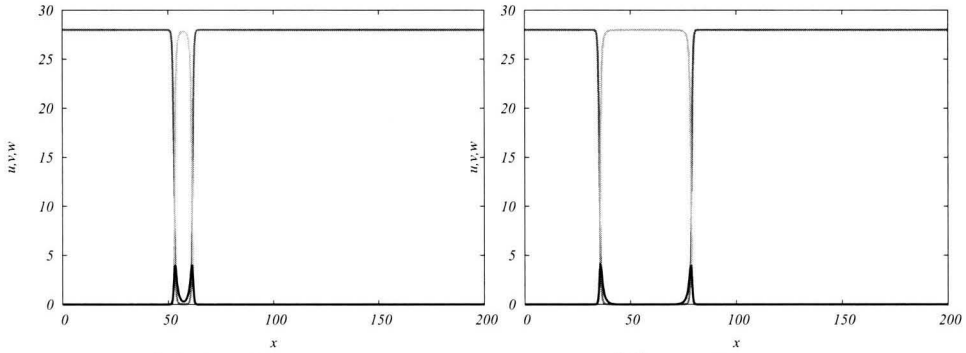

(c) $t = 20$ (d) $t = 33$

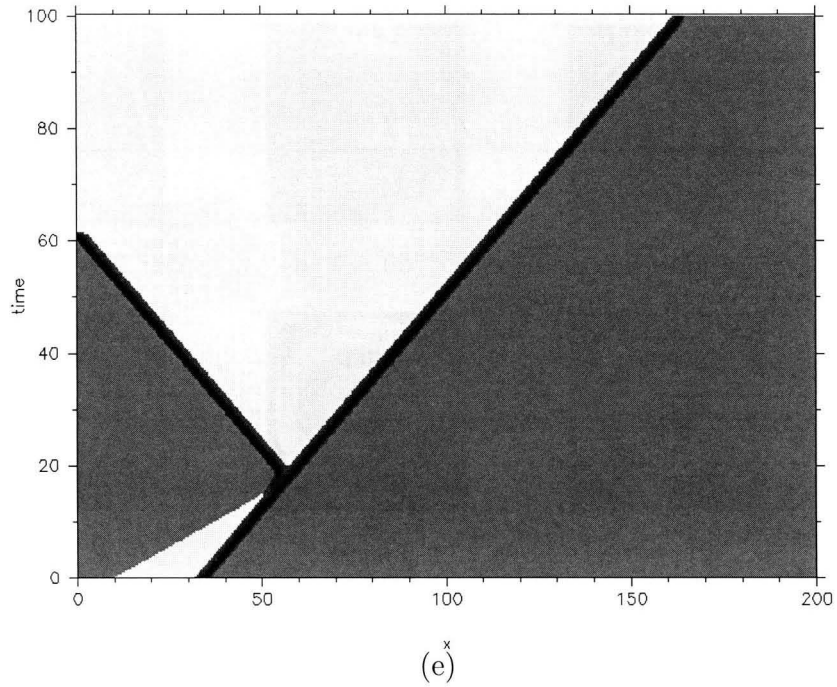

(e)

Figure 6.2: Interaction of two species- and three- species traveling wave solutions of (2.1)–(2.3) in one dimension where the parameters are specified to satisfy (3.1) and $b_{23} = 0.4$. Dark gray, light gray and black colors indicate the areas occupied by U, V and W, respectively.

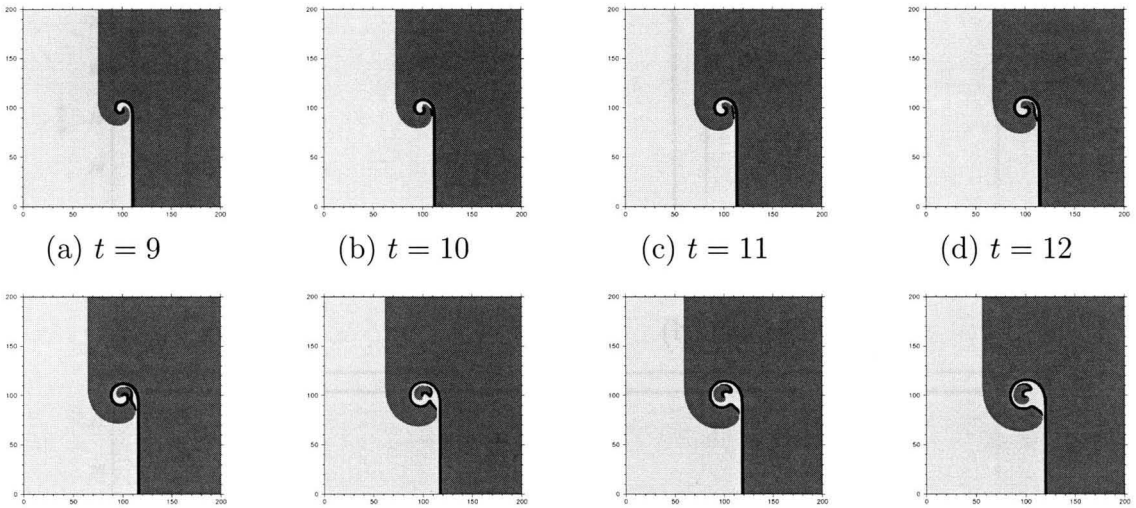

(a) $t = 9$ (b) $t = 10$ (c) $t = 11$ (d) $t = 12$

(e) $t = 13$ (f) $t = 14$ (g) $t = 15$ (h) $t = 16$

Figure 6.3: Dynamics of a solution of (2.1)–(2.3) where parameters are the same as in Figure 5.3. Dark gray, light gray, and black colors indicate the areas occupied by U, V and W, respectively.

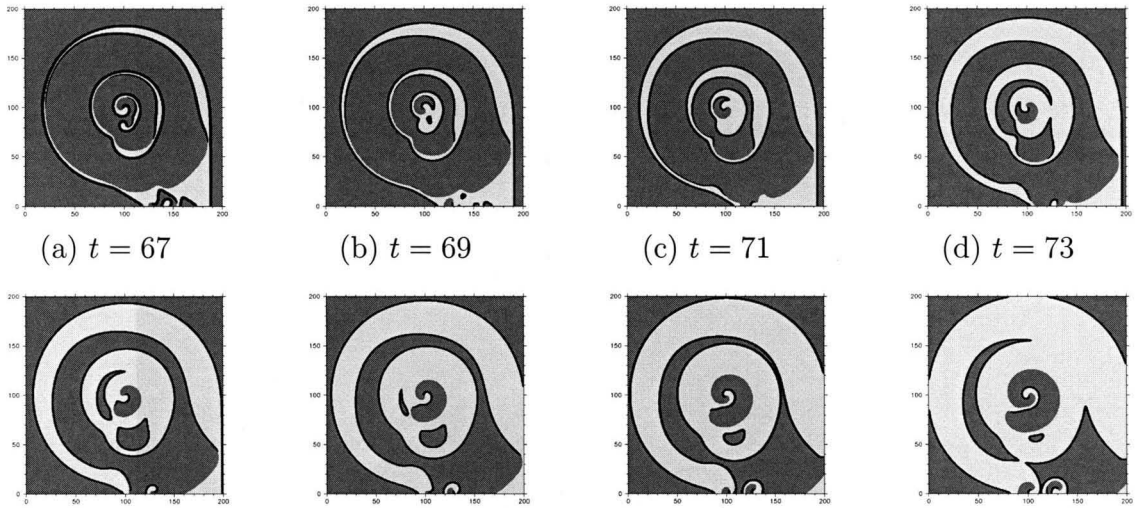

(a) $t = 67$ (b) $t = 69$ (c) $t = 71$ (d) $t = 73$

(e) $t = 75$ (f) $t = 77$ (g) $t = 79$ (h) $t = 81$

Figure 6.4: Dynamics of a solution of (2.1)–(2.3) where parameters are the same as in Figure 5.3. Dark gray, light gray, and black colors indicate the areas occupied by U, V and W, respectively.

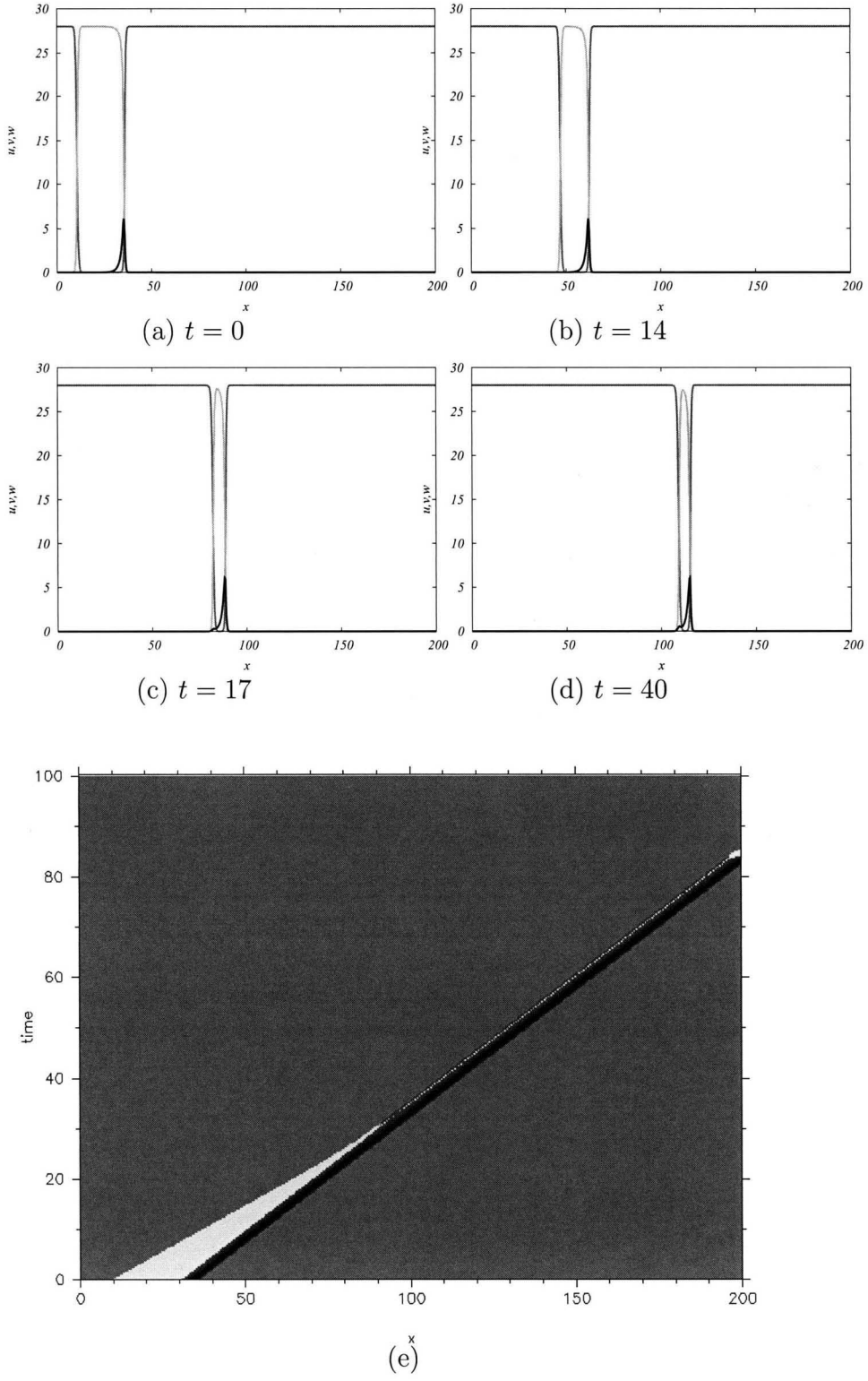

Figure 6.5: Occurrence of one dimensional homoclinic type traveling wave solution of (2.1)–(2.3), where the parameters are specified to satisfy (3.1) and $b_{23} = 0.6$. Dark gray, light gray and black colors indicate the areas occupied by U, V and W, respectively.

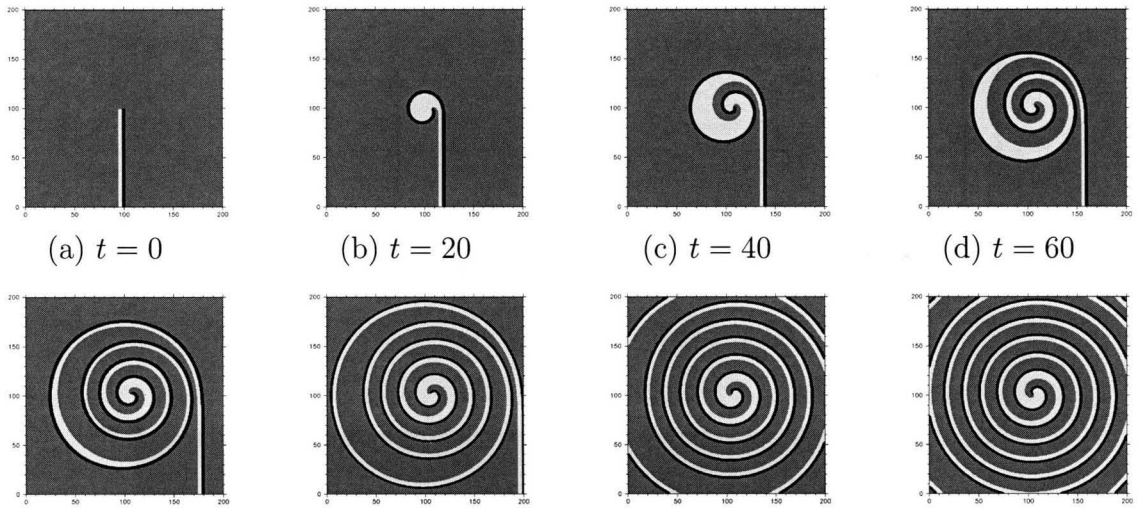

(a) $t = 0$ (b) $t = 20$ (c) $t = 40$ (d) $t = 60$

(a) $t = 80$ (b) $t = 100$ (c) $t = 120$ (d) $t = 140$

Figure 6.6: Occurrence of steadily rotating spirals. Here the initial functions where the three species homoclinic traveling wave solution locates in lower region of Ω where the parameters are specified to satisfy (3.1) and $b_{23} = 0.6$. Dark gray, light gray and black colors indicate the areas occupied by U, V and W, respectively.

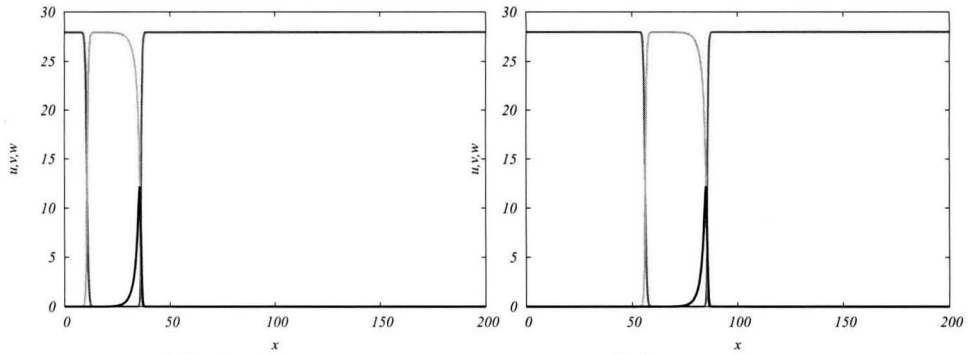

(a) $t = 0$ (b) $t = 18$

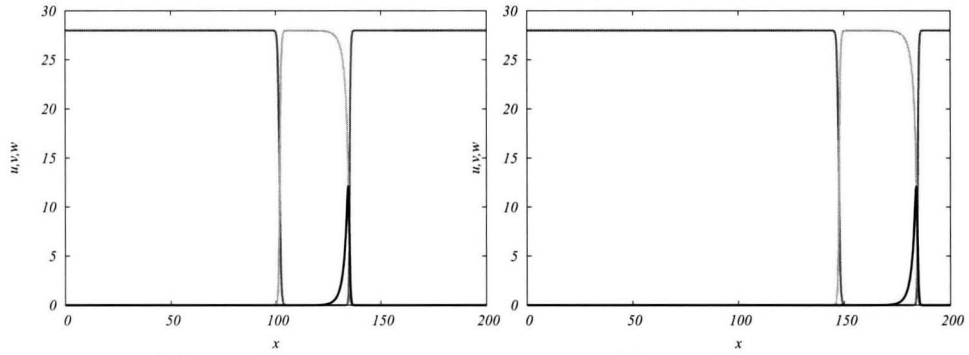

(c) $t = 33$ (d) $t = 50$

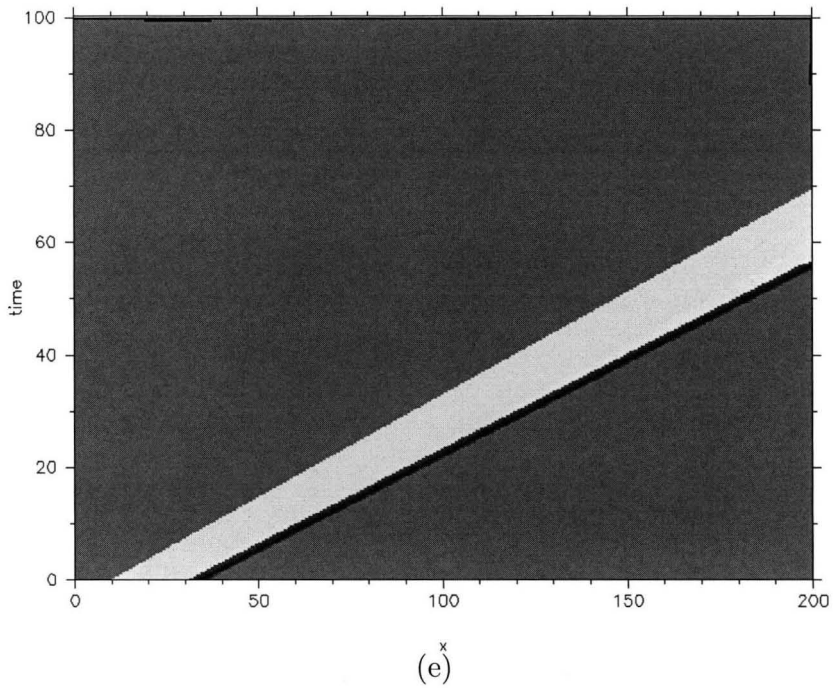

(e)

Figure 6.7: Interaction of two species- and three- species traveling wave solutions of (2.1)–(2.3) in one dimension where the parameters are specified to satisfy (3.1) and $b_{23} = 0.8$. Dark gray, light gray and black colors indicate the areas occupied by U, V and W, respectively.

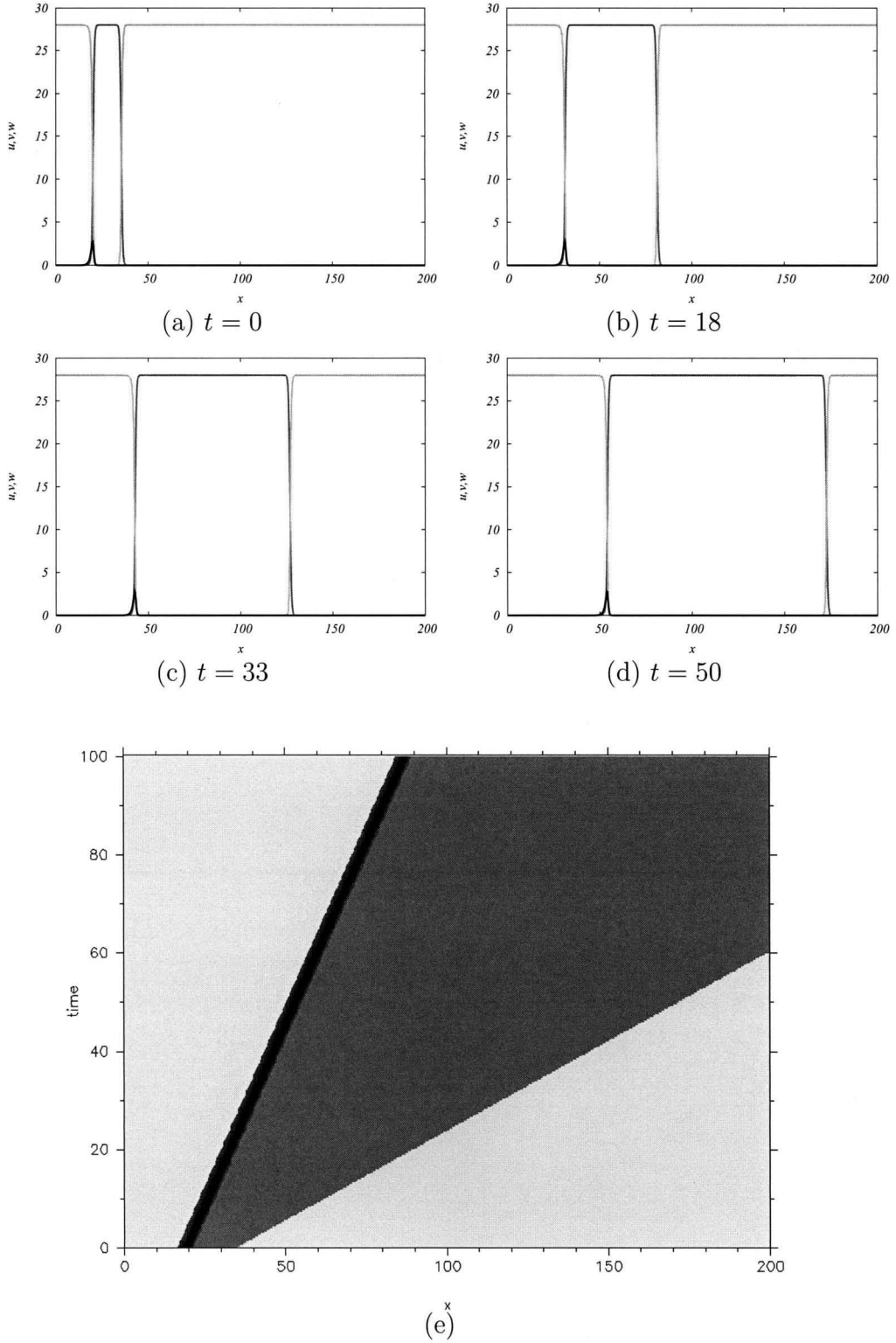

(a) $t = 0$ (b) $t = 18$

(c) $t = 33$ (d) $t = 50$

(e)

Figure 6.8: Interaction of two species- and three- species traveling wave solutions of (2.1)–(2.3) in one dimension where the parameters are specified to satisfy (3.1) and $b_{23} = 0.2$. Dark gray, light gray and black colors indicate the areas occupied by U, V and W, respectively.

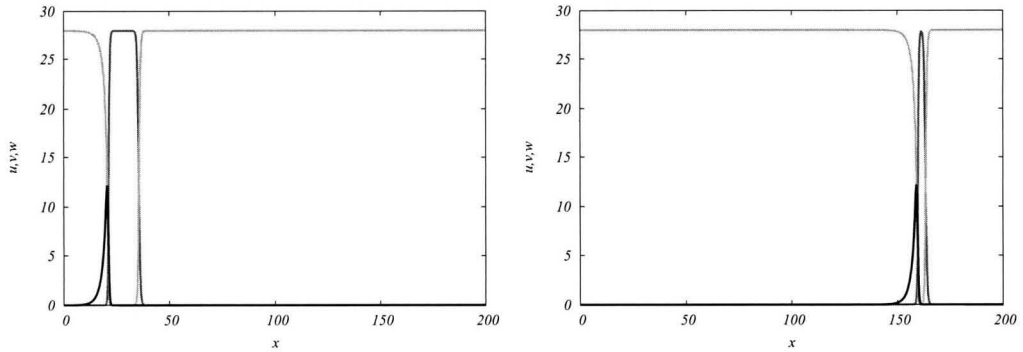

(a) $t = 0$ (b) $t = 27$

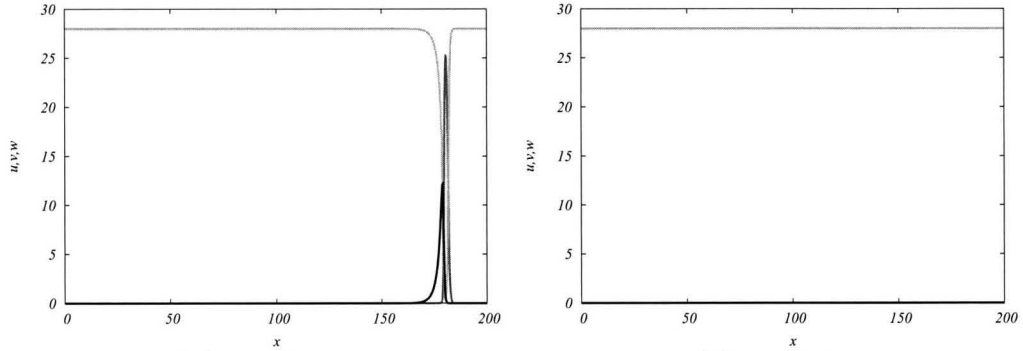

(c) $t = 53$ (d) $t = 60$

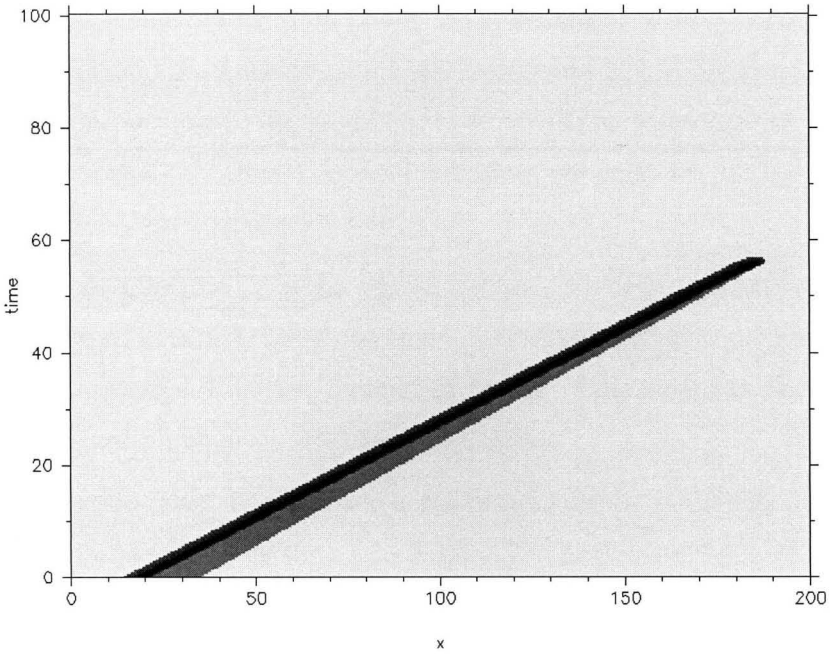

(e)

Figure 6.9: Interaction of two species- and three- species traveling wave solutions of (2.1)–(2.3) in one dimension where the parameters are specified to satisfy (3.1) and $b_{23} = 0.8$. Dark gray, light gray and black colors indicate the areas occupied by U, V and W, respectively.

Chapter 7

Occurrence of steadily rotating spirals

In the Chapter 6, I showed numerically that when one dimensional homoclinic type traveling wave solutions of (4.1) and (6.1) exist, steadily rotating spiral pattern occurs in two dimensions, as shown in Figure 6.6. Unfortunately, I have not yet proven the existence of homoclinic traveling wave solutions of (4.1) and (6.1). However, I can numerically obtain the branch of homoclinic traveling wave solutions of (4.1) and (6.1) in some interval of b_{23} (approximately $0.49\ldots < b_{23} < 0.75\ldots$), as shown in Figure 7.1. As shown in Figures 6.2 and 6.7, if b_{23} is relatively small or large, stable homoclinic traveling wave solutions seem not to occur. This suggests that homoclinic traveling wave solutions are exist for limited range of b_{23}. It is numerically shown that such solutions .

As shown in Figure 6.2, when $b_{23} < 0.49\ldots$, if three species traveling wave approaches two species one, there appears a new three species traveling wave which moves to the opposite direction instead of fusing. This suggests that homoclinic traveling wave solutions are unstable even if exist.

Next, I discuss what happen when b_{23} is near $0.75\ldots$. When $b_{23} = 0.7$, the core radius becomes large as shown in Figure 7.2, and when $b_{23} = 0.735$, the core radius becomes too large to appear any spiral but a rotating spiral arm remains, as shown in Figure 7.3, where the corresponding core radii are shown in Figures 7.5 and 7.6, respectively. The dependency of core radius of rotating spiral on b_{23} is shown in Figure 7.7.

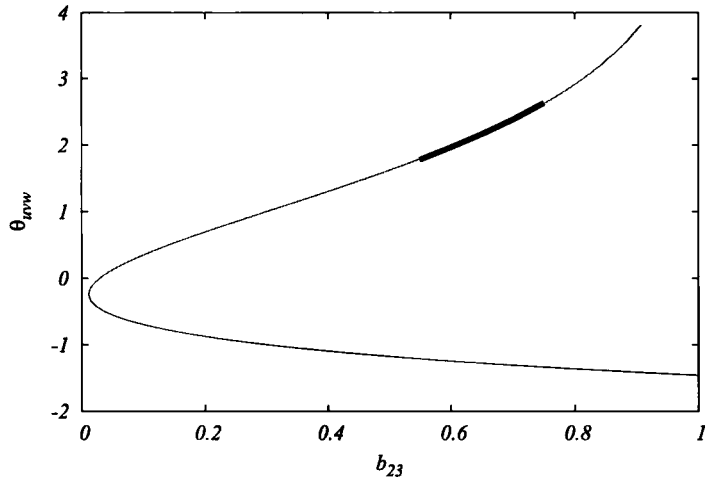

Figure 7.1: Global structure of homoclinic traveling wave solutions when b_{23} is varied where d_i, r_i, a_i and $b_{i,j}(i,j = 1,2,3(i \neq j))$ are specified to satisfy (3.1). Black solid line represents a homoclinic type traveling wave solution of (4.1) and (6.1).

I first note that the spiral arms in Figures 7.4 – 7.6 is not the homoclinic traveling wave solutions, because the boundary conditions of the traveling wave solutions are (6.1), in other words, the traveling wave is moving in region of U, but the spiral arm is moving in region of V as shown in Figure 7.4. In other words, front wave of the spiral arm consists of two species which is faster and back one consists of three species which is slower. This suggests that the scenario of occurrence of the steadily rotating spiral pattern in (2.1)–(2.3) is not similar to the scenario of occurrence of rotating spirals of the Belousov-Zhabotinsky reaction ([32]) .

To examine the spiral arm, I investigate initial stage of $b_{23} = 0.735$ in Figure 7.8, which indicates that two species traveling wave which is faster and three species one which is slower are attached to each other and the core is the attached point, and the core moves in a circular pattern to absorb the difference of speed. Furthermore, it seems that the smaller the velocity difference is, the larger the core radius becomes because the difference to be absorbed becomes small, too. When the core radius is large,distance between the spiral arms is also large as shown in

Figures 7.2 and 7.3. So, the interaction between the spiral arms can not occur near core. But, because the front wave (resp. back wave) of the spiral arm is corresponding to the two species (resp. three species) traveling wave, the front wave approaches to the back wave of former spiral arm, and homoclinic traveling wave like behavior appears as if it is the arm of rotating spiral.

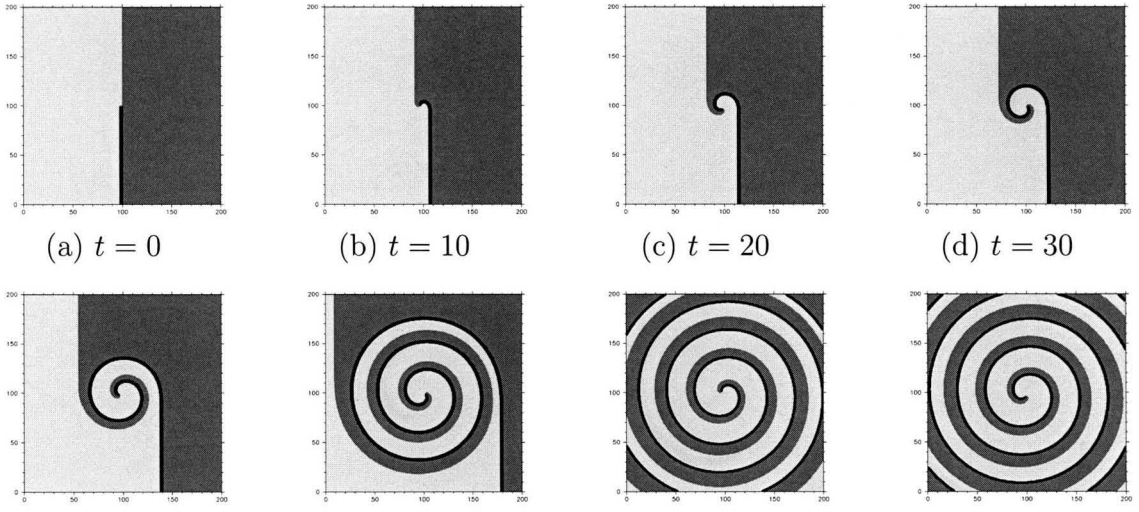

(a) $t = 0$ (b) $t = 10$ (c) $t = 20$ (d) $t = 30$

(e) $t = 50$ (f) $t = 100$ (g) $t = 150$ (h) $t = 200$

Figure 7.2: Occurrence of a rotating spiral in (2.1)–(2.3) where d_i, r_i, a_i and $b_{i,j}(i, j = 1, 2, 3(i \neq j))$ satisfy (3.1) and $b_{23} = 0.70$. Dark gray, light gray, and black colors indicate the areas occupied by U, V, and W, respectively.

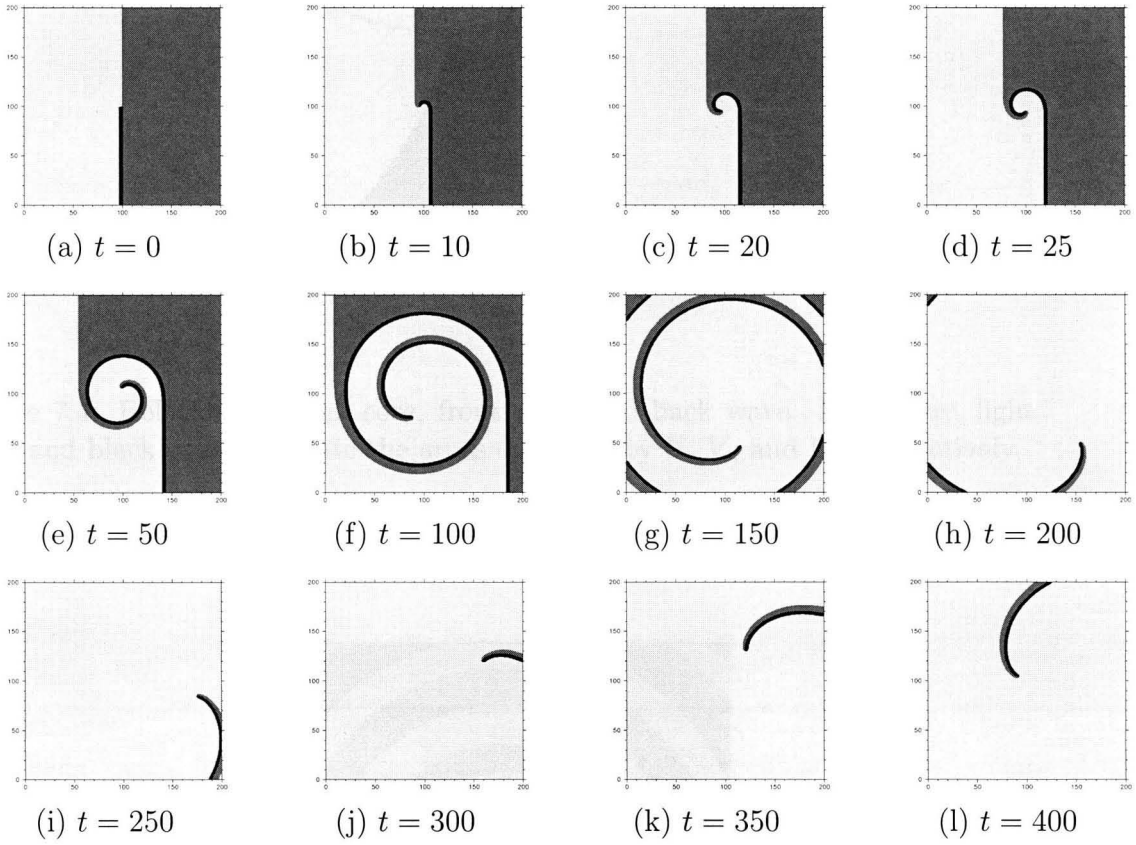

(a) $t = 0$ (b) $t = 10$ (c) $t = 20$ (d) $t = 25$

(e) $t = 50$ (f) $t = 100$ (g) $t = 150$ (h) $t = 200$

(i) $t = 250$ (j) $t = 300$ (k) $t = 350$ (l) $t = 400$

Figure 7.3: The core radius becomes too large to appear any spiral in (2.1)–(2.3) where d_i, r_i, a_i and $b_{i,j}(i, j = 1, 2, 3(i \neq j))$ satisfy (3.1) and $b_{23} = 0.735$. Dark gray, light gray, and black colors indicate the areas occupied by U, V, and W, respectively.

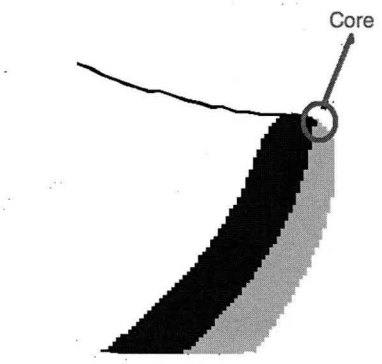

Figure 7.4: Relation between core, front wave and back wave. Dark gray, light gray, and black colors indicate the areas occupied by U, V, and W, respectively.

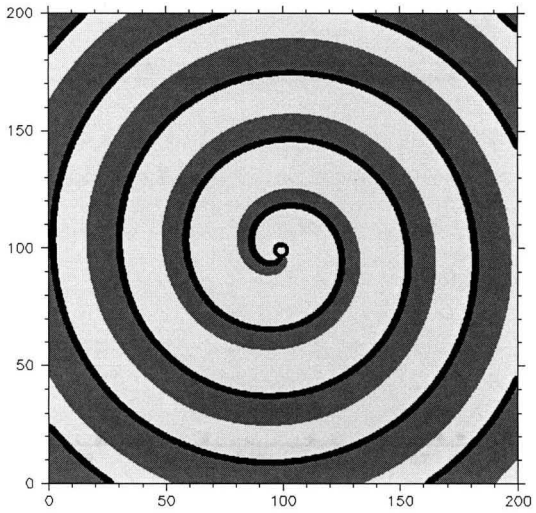

Figure 7.5: Tragectory of spiral core in Figures 7.2 ($b_{23} = 0.70$)

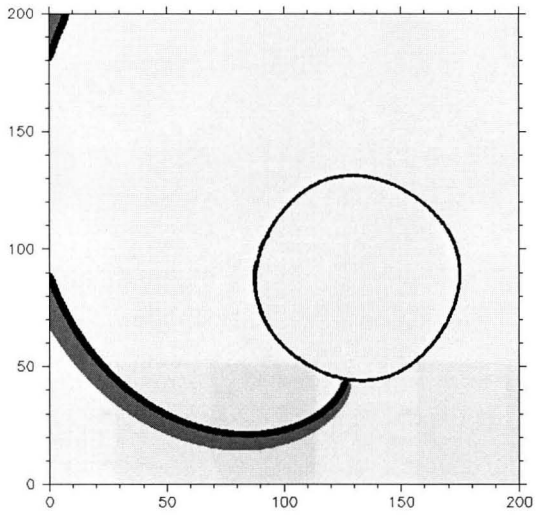

Figure 7.6: Tragectory of spiral core in Figures 7.3 ($b_{23} = 0.735$)

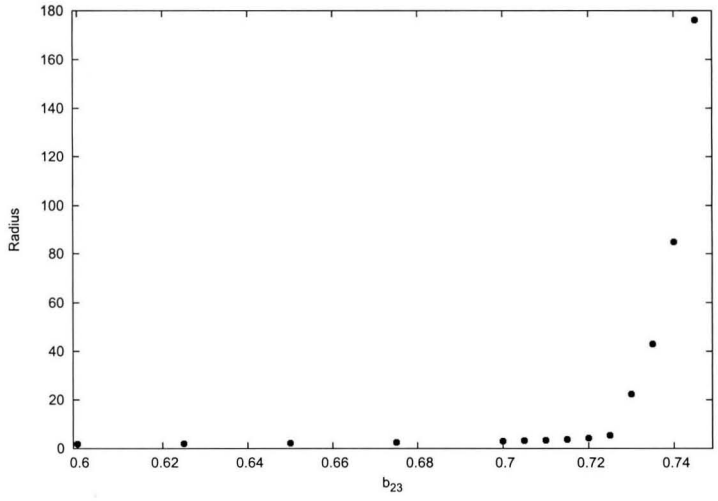

Figure 7.7: Dependency of b_{23} on the core radius of spirals in (2.1) where b_{23} is varied.

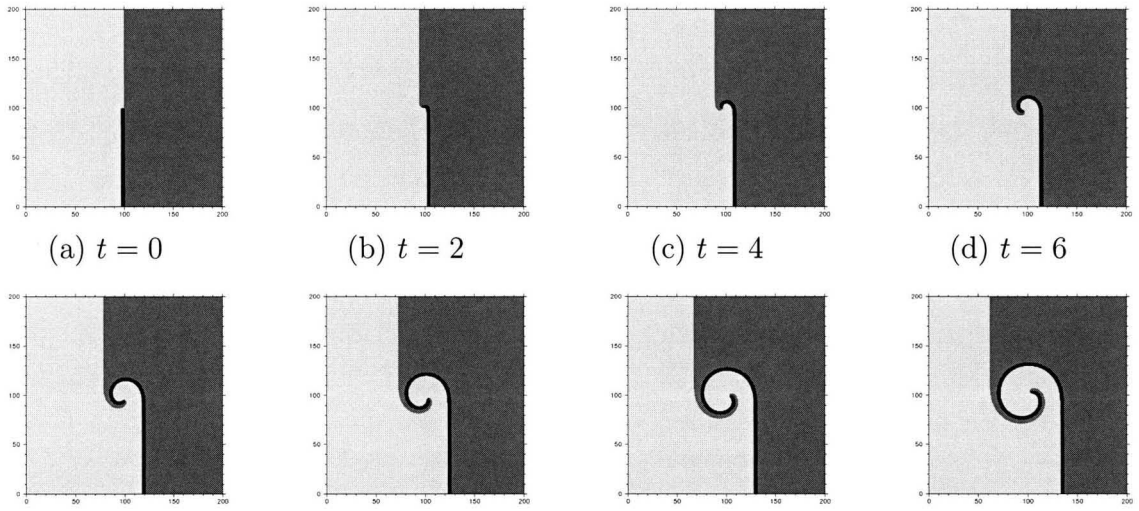

(a) $t = 0$ (b) $t = 2$ (c) $t = 4$ (d) $t = 6$

(e) $t = 24$ (f) $t = 30$ (g) $t = 36$ (h) $t = 42$

Figure 7.8: Initial stage of(2.1)–(2.3) where parameters are the same in Figure 7.3. Dark gray, light gray, and black colors indicate the areas occupied by U, V, and W, respectively.

Chapter 8

Wedge–shaped traveling wave solutions

As shown in Figure 5.5, when $b_{23} = 0.8$, the front wave moves rather faster than the back one, and spiral patterns do not occurs any more and it seems that the resulting pattern is described by a superposition of a planar wave of two species moving to the left direction and a radially symmetric expanding disk of three species. As shown in Figure 8.1, the tip moves to a certain fixed direction after some time.

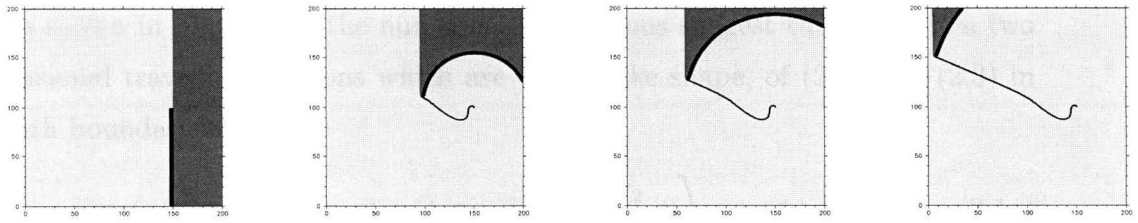

(a) $t = 0$ (b) $t = 20$ (c) $t = 33$ (d) $t = 53$

Figure 8.1: Interaction of two species- and three species- traveling wave solution of (2.1)–(2.3) becomes planar wave of two species moving to the left direction and the radially symmetric expanding disk of three species. d_i, r_i, a_i and $b_{i,j}(i, j = 1, 2, 3(i \neq j))$ satisfy (3.1) except $b_{23} = 0.8$. Dark gray, light gray and black indicate the area occupied by U, V, and W, respectively and black line indicate the trajectory of core.

Figure 8.1 suggests that if this behavior is considered in the whole plane $\mathbb{R}^2$, a superposition of a planar traveling wave and a radially symmetric expanding disk

tends to a superposition of two planar traveling waves after large time. In other words, one can expect that there is a wedge–shaped traveling wave solution which consists of a superposition of two planar traveling waves of two and three species.

To confirm this expectation, I take the initial conditions $(u_0(x,y), v_0(x,y), w_0(x,y))$ in square domain Ω as a superposition of two planar traveling waves, as shown in Figure 8.2 (a).

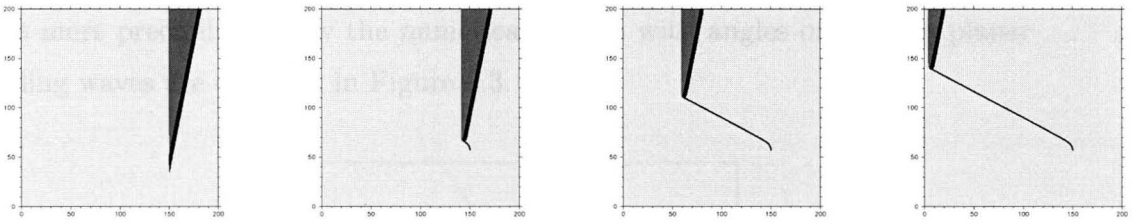

(a) $t = 0$ (b) $t = 3$ (c) $t = 33$ (d) $t = 53$

Figure 8.2: Superposition of two and three species traveling plane wave solutions of (2.1)–(2.3) where d_i, r_i, a_i and $b_{i,j}(i,j = 1,2,3(i \neq j))$ satisfy (3.1) except $b_{23} = 0.8$. Dark gray, light gray and black indicate the area occupied by U, V, and W, respectively and black line indicate the trajectory of core.

As shown in Figure 8.2, the numerical simulations suggest that there is a two dimensional traveling solutions which are wedge–like shape, of (2.1) and (2.3) in $\mathbb{R}^2$ with boundary condition

$$\lim_{x\to\pm\infty}(u(t,x,y), v(t,x,y), w(t,x,y)) = \left(0, \frac{r_2}{a_2}, 0\right), \qquad t > 0, \tag{8.1a}$$

$$\lim_{y\to\infty}(u(t,x,y), v(t,x,y), w(t,x,y)) = (\hat{u}(t,x), \hat{v}(t,x), 0), \qquad t > 0, \tag{8.1b}$$

$$\lim_{y\to-\infty}(u(t,x,y), v(t,x,y), w(t,x,y)) = \left(0, \frac{r_2}{a_2}, 0\right), \qquad t > 0, \tag{8.1c}$$

where $(\hat{u}(t,x), \hat{v}(t,x), 0)$ is the one dimensional two species traveling wave solution. I named this two dimensional traveling wave solutions *wedge–shaped traveling wave solutions.*

The wedge–shaped traveling wave solutions can be understood as follows: As shown in Figure 6.9, in one dimensional problem, the back wave which consists of three species approaches from behind of the front one which consists of two

species, and they annihilate each other when they collide. Consider what happen when the three species planar traveling wave approaches from diagonally behind to the two species one. One can expect that the annihilation occurs only at the intersection of the front and back waves, and superposition of the two species- and three species- traveling waves forms wedge like shape and moves with fixed velocity depends on the planar traveling ones.

To understand the superposition of the two species- and three species- traveling waves more precisely, I show the numerical results with angles of the two planar traveling waves are different in Figure 8.3.

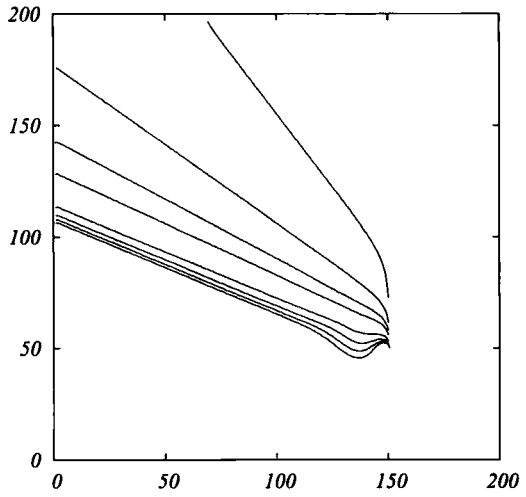

Figure 8.3: The trajectory of tip when angle between two planar traveling waves change. The lines beginning at the top indicate the trajectory which the angle of initial state is $\pi/48, \pi/24, \pi/16, \pi/12, \pi/6, \pi/4, \pi/3, 5\pi/12$, respectively

Now, I conjecture the following:

Conjecture 8.1. *There is some critical angle η_c such such that for any η satisfying $0 < \eta < \eta_c$, there is a wedge-like traveling wave solutions (u, v, w) where the front and back waves are given by the two and three species planar traveling waves where η is the angle between two traveling waves.*

To support Conjecture 8.1, I first discuss about a superposition of moving two straight lines, which corresponds to a situation without diffusion effect. Along this

line of discussion, I first state the following proposition about a superposition of moving two straight lines:

Proposition 8.2. *Consider two straight lines L_F and L_B moving with velocity $V_F, V_B (V_F \leq V_B)$, respectively, as shown in Figure 8.4. If the angle between L_F, L_B is η, the angle between the trajectory of intersection and the direction perpendicular to L_B is given by*

$$\tan^{-1}\left(\frac{\cos(\eta) - V_F/V_B}{\sin(\eta)}\right). \tag{8.2}$$

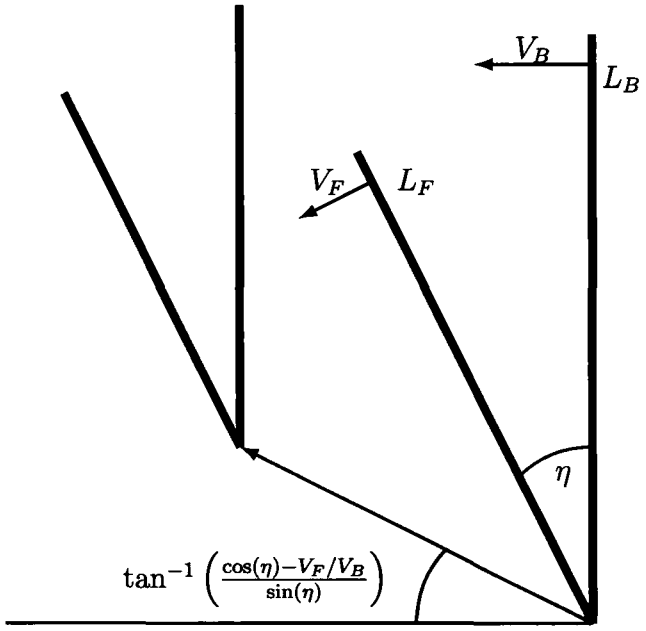

Figure 8.4: Relation between L_B, L_F and η in Proposition 8.2

I show the proof of Proposition 8.2 in Appendix.

From Proposition 8.2, I can show following corollary:

Corollary 8.3. *Suppose η_v is the angle η when the intersection moves in a direction perpendicular to L_B,*

$$V_F = \cos(\eta_v) V_B. \tag{8.3}$$

Proof. The proof is so obvious from (8.2) that I omit it. □

Next, I discuss when the straight lines exhibit the change of species like as the two species- and three species- traveling waves. Consider the area passed by L_F is occupied by U and L_B wipes out U. As shown in Figure 8.5 (a), when $0 < \eta < \eta_v$, U occupies the moving wedge shaped area only. On the other hand, as shown in Figure 8.5 (b), when $\eta > \eta_v$, U also remains a triangle shaped area.

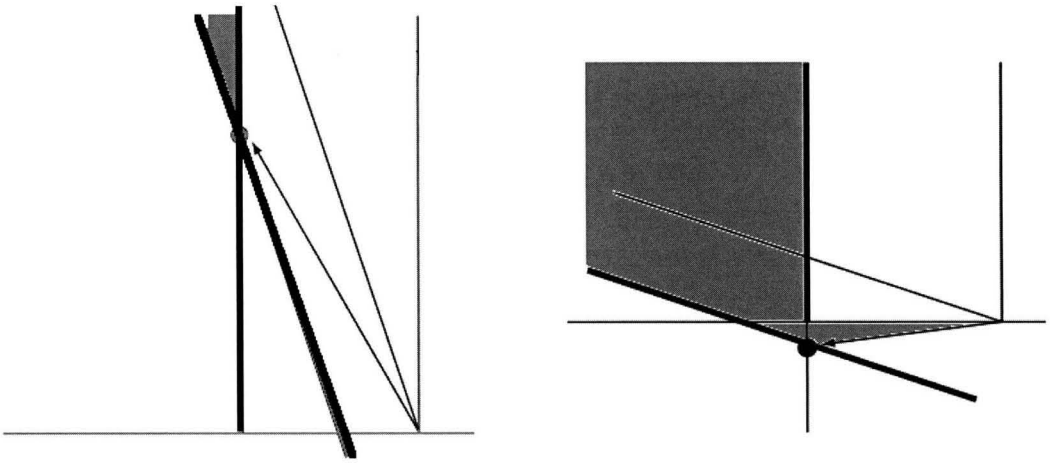

(a) $\eta < \eta_v$ (b) $\eta > \eta_v$

Figure 8.5: Region occupied by U without diffusion effect

From Figure 8.5 (a), one can expect that when $0 < \eta < \eta_v$, the wedge shape traveling wave solution appears even if diffusion effect exists. In addition, one can expect from Figure 8.5 (b) that the tip of wedge bend to absorb the triangle, and when the angle to tip become η_v, the bending stops and the tip moves to fixed direction. This expectancy is supported by numerical results as shown in Figure 8.6. These expectancies have good agreements with Figure 8.3 and support Conjecture 8.1 with $\eta_c = \eta_v = \cos^{-1}(V_F/V_B)$.

In order to confirm the validity of above discussion quantitatively, I verify whether or not the angle predicted from (8.2) agrees with the actual measured value. In Figure 8.2, the speed of front wave V_F is $|\theta_{uv}| = 2.57\ldots$ and the speed of back wave V_B is $|\theta_{uvw}| = 2.92\ldots$, and the angle between the two planar traveling wave solutions is $\eta = 0.20$, so the calculated angle is

$$\frac{\cos(0.20) - (2.57/2.92)}{\sin(0.20)} = 0.51\ldots \tag{8.4}$$

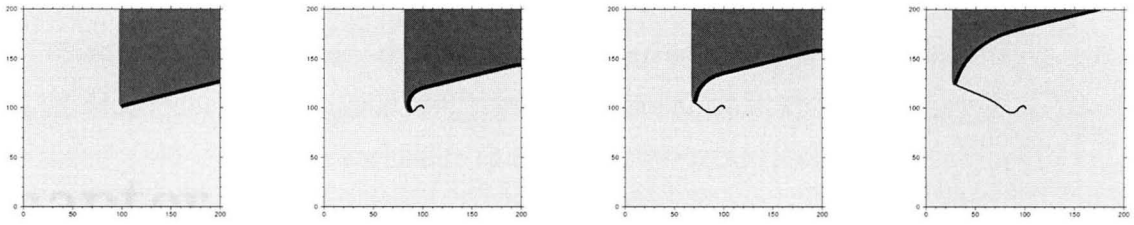

(a) $t = 0$ (b) $t = 6$ (c) $t = 11$ (d) $t = 26$

Figure 8.6: Superposition of two species- and three species- traveling wave solutions of (2.1)–(2.3) where d_i, r_i, a_i and $b_{i,j}(i, j = 1, 2, 3(i \neq j))$ satisfy (3.1) and $b_{23} = 0.8$. Dark gray, light gray and black indicate the area occupied by U, V, and W, respectively and black line indicate the trajectory of core.

which is a good agreement with to the actual angle $0.54\ldots$.

Next, I discuss about the situation that back wave is three species radially symmetric expanding traveling wave, as shown in Figure 5.5. In this case, if the collision angle is small, the angle that allows the tip of the wedge to move in the direction perpendicular to back wave so the angle becomes large, whereas if the angle is large, the tip moves in the direction of back wave moving, so the angle becomes small. So one can expect that a fixed angle will be selected as a result. From Corollary 8.3, one can expect that the fixed angle is given by $\eta_c = \cos^{-1}(\theta_{uv}/\theta_{uvw})$.

In order to confirm the validity of the expectancy quantitatively, I compare the angle predicted from (8.3) with the actual measured value in the case of Figure 5.5. In this case, calculated angle is

$$\eta = \cos^{-1}\left(\frac{\theta_{uv}}{\theta_{uvw}}\right) = 0.49 \tag{8.5}$$

which is a good agreement with to the actual angle $0.45\ldots$. This demonstrates the validity of the approximation in this case, too.

Chapter 9

Concluding remarks

In Chapter 1, I stated the problem: *First, consider the situation in which there is a two native species system, where one is stronger than the other in competition, that is, competitive exclusion occurs between them. Second, consider a situation in which a single exotic competing species invades the native system. Is it possible for the modified system of two native species and one exotic species to coexist, even if the exotic species is relatively weaker than either of the native species?*

By using a three species competition–diffusion system (2.1)–(2.3), I can say "Yes", for a suitable parameter range in the system. In other words, It has been shown that competitor-mediated coexistence can occur by exotic species for a suitable parameter range, even if the exotic species is weak.

However, the behaviors are sensitive to the value of the parameter b_{23} which represents the relation between the exotic species and the weaker native species. In Chapter 3, it was demonstrated that three types of asymptotic behaviors arise depending on the value of b_{23}, even if the exotic species W can survive only in the vicinity of the boundary between the two strongly competing native species. The three types of asymptotic behaviors are as follows: (a) the exotic species fades out, but the competitive relation of the native species is reversed so that the stronger native species can not survive, (b1) the exotic species survives, and competitor–mediated coexistence exhibiting complex spatio-temporal pattern occurs, (b2) the exotic species survives, and competitor–mediated coexistence exhibiting steadily rotating spirals occurs. In addition, it was shown that the one dimensional two species- and three species- traveling wave solutions provide essential information

on the occurrence or non-occurrence of competitor–mediated coexistence.

In Chapter 4, To examine the behaviors of two species- and three species-traveling waves, it was shown that the interaction between the traveling waves can be classified with respect to the value of the parameter b_{23} into three types: (I) collision and reflection, (II) collision and fusion, (III) collision and annihilation.

In Chapter 6, it was demonstrated that the three types of asymptotic behavior can be explained from the classification of interactions between the traveling waves as follows: (A) when the three species traveling wave solutions are faster than the two species ones, competitor–mediated coexistence does not occur, but the competitive relation of native species is reversed so that the stronger native species can not survive, (B1) when the three species traveling wave solutions is slower than the two species ones and the interaction between these two traveling waves are "collision and fusion", competitor–mediated coexistence exhibiting steadily rotating spirals occurs, (B2) when the three species traveling wave solutions are slower than the two species ones and the interaction between the traveling waves is "collision and reflection", there are two types of asymptotic behaviors. It was shown that the two types of asymptotic behaviors given in class (B2) are as follows: (B2a) competitive exclusion with reverse of the competitive relation of the native species, (B2b) competitor–mediated coexistence with complex spatio-temporal patterns. The asymptotic behavior (B2a) occurs when the difference of speeds of the two traveling waves is large, while that of (B2b) occurs when the difference is small.

Unfortunately, this sensitivity is not yet fully understood, although it is caused by the following three factors:

(i) planar stability of one dimensional two species traveling wave solutions and three species ones,

(ii) interaction between these two one dimensional traveling wave solutions; and

(iii) difference of speeds between these two one dimensional traveling wave solutions.

In Chapter 7, the steadily rotating spirals were investigated. The relation

between the spiral arms and fused homoclinic traveling waves, the parameter dependency of core radii in the steadily rotating spirals , and the reason why the core radii become large as the difference speeds of traveling waves tends to 0 were discussed. In addition, it was shown steadily rotating spiral can be understood from the three abovementioned factors (i)-(iii).

In Chapter 8, newly-discovered two dimensional traveling wave solutions which were named wedge–shaped traveling wave solutions were discussed. It was shown and confirmed quantitatively that these traveling solutions can be understood as a superposition of two planar traveling waves. It was shown that wedge–shaped traveling wave solutions can be understood from the three factors (i)-(iii), too.

Finally, the ecological significance of this study is evaluted. The fact that an exotic species cannot survive in a diffusionless system implies that such a species cannot survive in a small area, such as an experimental farm. However, on the basis of the model presented in the study, an exotic species can alter the conditions inherent within a strongly competing two species system even if it can survive only in the vicinity of the boundary between the two strongly competing native species, and it cannot coexist with the native species in a small area. This suggests that, when studying the influence of exotic species, experiments should be conducted over a wide area and attention should be paid to the relations between weak species.

Appendix Proof of Proposition 8.2

In this chapter, I show the proof of Proposition 8.2.

Proof. Without loss of generality, I can set that the intersection of L_B and L_F at the time $t = 0$ is taken to the origin of the coordinate system and L_B to overlap the Y axis as shown in Figure A.1.

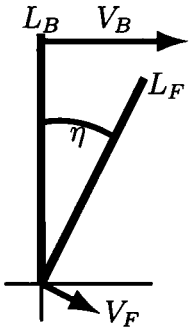

Figure A.1: Initial position of L_B and L_F

First, I determine the equation of L_F at the time $t = t_1$. Because the angle formed by the traveling direction of L_F with the X axis to be η, and the speed of L_F is V_F, x-intercept and y-intercept at $t = t_1$ will be $t_1 V_F / \cos(\eta)$ and $-t_1 V_F / \sin(\eta)$, respectively. Therefore, the equation of L_F at $t = t_1$ can be described as

$$y = \frac{x\cos(\eta) - t_1 V_F}{\sin(\eta)}. \tag{A.1}$$

With (A.1), the intersection of L_B and L_F can be described as

$$(t_1 V_B, \frac{t_1 V_B \cos(\eta) - t_1 V_F}{\sin(\eta)}). \tag{A.2}$$

With (A.2), the equation of the trajectory of intersection can be described as

$$y = \frac{\cos(\eta) - V_F/V_B}{\sin(\eta)} x, \tag{A.3}$$

as showin in Figure A.2. So, I can conclude that the angle between trajectory of intersection and the direction perpendicular to L_B is given by

$$\tan^{-1}\left(\frac{\cos(\eta) - V_F/V_B}{\sin(\eta)}\right).$$

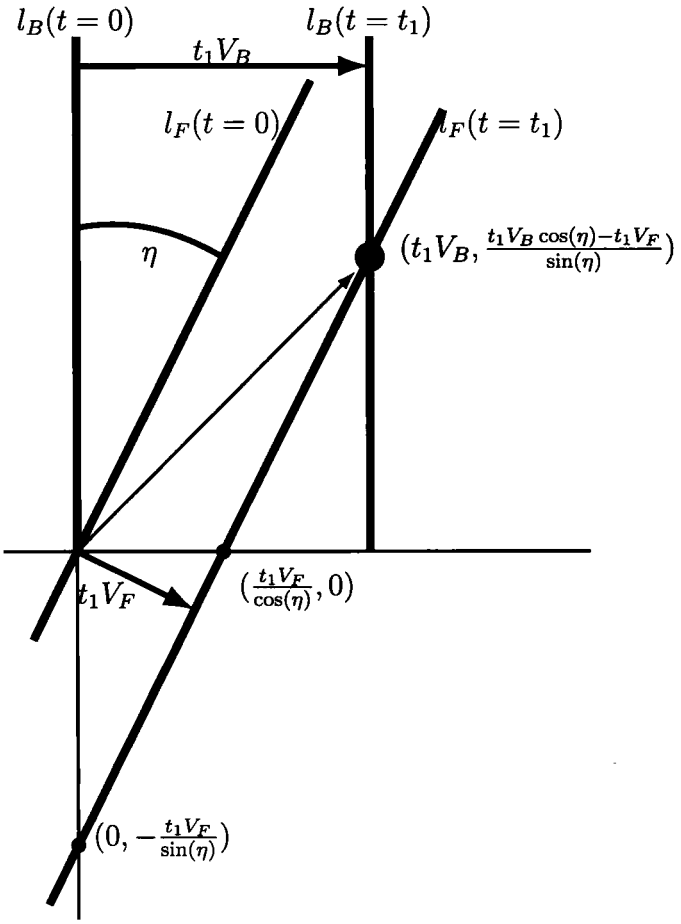

Figure A.2: Positions of the lines and intersection at $t = 0$ and $t = t_1$

□

Publications

Refereed papers published in journals or books

- C.-C. Chen, L.-C. Hung, M. Mimura, M. Tohma, and D. Ueyama: Semi-exact equilibrium solutions for three-species competition-diffusion systems, to appear in Hiroshima Mathematical Journal.

Un-refereed papers published in local conference proceedings

- M. Mimura, and M. Tohma : Dynamic spiral coexistence in competing species, Annual Conference of The Japan Society for Industrial and Applied Mathematics 2012 (in Japanese).

Bibliography

[1] A. Arneodo, P. Coullet, and C. Tresser. Strange attractors in Volterra equations for species in competition. *Journal of Mathematical Biology*, 14:153–157, 1982.

[2] C.-C. Chen, L.-C. Hung, M. Mimura, M. Tohma, and D. Ueyama. Semi-exact equilibrium solutions for three-species competition-diffusion systems. *to appear in Hiroshima Mathematical Journal.*

[3] C.-C. Chen, L.-C. Hung, M. Mimura, and D. Ueyama. Exact traveling wave solutions of three species competition-diffusion systems. *to appear in Discrete and Continuous Dynamical Systems B.*

[4] E. Conway, D. Hoff, and J. Smoller. Large time behavior of solutions of systems of nonlinear reaction-diffusion equations. *SIAM J. Appl. Math.*, 35(1):1–16, 1978.

[5] J. M. Cushing. Two species competition in a periodic enviroment. *J. Math. Biol*, 10:385–400, 1980.

[6] P. de Mottoni and A. Schiaffino. Competition systems with periodic coefficients: a geometric approach. *Journal of Mathematical Biology*, 11:315–335, 1981.

[7] E. J. Doedel, B. E. Oldeman, A. R. Champneys, F. Dercole, T. F. Fairgrieve, , Y. Kuznetsov, R. C. Paffenroth, B. Sandstede, X. J. Wang, and C. H. Zhang. Auto-07p: Continuation and bifurcation software for ordinary differential equations. version 0.7, `http://sourceforge.net/projects/auto-07p/files/auto07p/`, 2010.

[8] S.-I. Ei, R. Ikota, and M. Mimura. Segregating partition problem in competition-diffusion systems. *J. Interfaces and Free Boundaries*, 1:57–80, 1999.

[9] S.-I. Ei and M. Mimura. Transient and large time behaviors of solutions to heterogeneous reaction-diffusion equations. *Hiroshima Mathematical Journal*, 14:649–678, 1984.

[10] G. F. Gause. *The Struggle for Existence.* The Williams & Wilkins Company, Baltimore, 1934.

[11] M. Gyllenberg, P. Yau, and Y. Wang. A 3D competitive Lotka-Volterra system with three limit cycles: A falsification of conjecture by Hofbauer and So. *Applied Mathematics Letters*, 19:1–7, 2006.

[12] M. W. Hirsch. Differential equations and convergence almost everywhere of strongly monotone semiflows. Technical report, University of California. Berkeley, 1982.

[13] M. W. Hirsch. Systems of differential equations which are competitive or cooperative:III competing species. *Nonlinearity*, 1:51–71, 1988.

[14] J. Hofbauer and J. W.-H. So. Multiple limit cycles for three dimensional Lotka-Volterra equations. *Appl. Math. Lett.*, 7(6):65–70, 1994.

[15] G. E. Hutchinson. The paradox of the plankton. *American Naturalist*, 95:134–143, 1961.

[16] H. Ikeda. Private Communication.

[17] Japan Wildlife Research Center. *A photographic guide to the invasive alien species in Japan.* Heibonsha, 2008.

[18] Y. Kan-on. Stability of singularly perturbed solutions to nonlinear diffusion systems arising in population dynamics. *Hiroshima Math. J.*, 23:509–536., 1993.

[19] Y. Kan-on. Parameter dependence of propagation speed of travelling waves for competition-diffusion equations. *SIAM J. Math. Anal.*, 26(2):340–363, 1995.

[20] Y. Kan-On and Q. Fang. Stability of monotone travelling waves for competition-diffusion equations. *Japan Journal of Industrial and Applied Mathematics*, 13:343–349, 1996.

[21] K. Kishimoto and H. F. Weinberger. The spatial homogeneity of stable equilibria of some reaction-diffusion systems on convex domains. *J. Differential Equations*, 58(1):15–21, 1985.

[22] X. Lian, Z. Lu, and Y. Luo. Automatic search for multiple limit cycles in three-dimensional Lotka–Volterra competitive systems with classes 30 and 31 in zeeman's classification. *Journal of Mathematical Analysis and Applications*, 348:34–37, 2008.

[23] Z. Lu and Y. Luo. Two limit cycles in three-dimensional Lotka-Volterra systems. *Computers and Mathematics with Applications*, 44:51–66, 2002.

[24] Z. Lu and Y. Luo. Three limit cycles for a three-dimensional Lotka-Volterra competitive system with a heteroclinic cycle. *Computers and Mathematics with Applications*, 46:231–238, 2003.

[25] H. Matano and M Mimura. Pattern formation in competition-diffusion systems in non convex domains. *Publ. RIMS, Kyoto Univ*, 19:1049–1079, 1983.

[26] R. M. May and W. J. Leonard. Nonlinear aspects of competition between three species. *SIAM J. Appl. Math.*, 29:243–253, 1975.

[27] M. Mimura. Stationary pattern of some density dependent diffusion system with competitive dynamics. *Hiroshima Math. J.*, 11:621–635, 1981.

[28] M. Mimura and K. Kawasaki. Spatial segragation in competitive interaction–diffusion equations. *Math. Biol.*, 9:49–64, 1980.

[29] M. Mimura, Y. Nishiura, A. Tesei, and T. Tsujikawa. Coexistence problem for two competing species models with density-dependent diffusion. *Hiroshima Math. J.*, 14:425–449, 1984.

[30] M. Rodrigo and M. Mimura. Exact solutions of reaction-diffusion systems and nonlinear wave equations. *Japan J. Indust. Appl. Math.*, 18(3):657–696, 2001.

[31] N. Shigesada, K. Kawasaki, and E. Teramoto. Spatial segregation of interacting species. *Journal of Theoretical Biology*, 79:83–99, 1979.

[32] T. Tsujikawa, T. Nagai, M. Mimura, R. Kobayashi, and H. Ikeda. Stability properties of traveling pulse solutions of the higher dimensional fitzhugh–nagumo equations. *Japan J. Appl. Math.*, 6:341–366, 1989.

[33] P. van den Driessche and M. L. Zeeman. Three-dimensional competitive Lotka-Volterra systems with no periodic orbits. *SIAM J. Appl. Math.*, 58(1):227–234, 1998.

[34] M. L. Zeeman. Hopf bifurcations in competitive three-dimensional Lotka-Volterra systems. *Dynam. Stability Systems*, 8(3):189–217, 1993.